Kinematic and thermal evolution of the Moroccan rifted continental margin: Doukkala-High Atlas Transect

Gouiza, M.; Bertotti, G.V.; Hafid, M.; Cloetingh, S.A.P.L.

published in
Tectonics
2010

DOI (link to publisher)
10.1029/2009TC002464

document version
Publisher's PDF, also known as Version of record

Kinematic and thermal evolution of the Moroccan rifted continental margin: Doukkala-High Atlas transect

M. Gouiza,[1,2] G. Bertotti,[1,2,3] M. Hafid,[4] and S. Cloetingh[1,2]

Received 11 February 2009; revised 13 March 2010; accepted 27 April 2010; published 15 September 2010.

[1] The Atlantic passive margin of Morocco developed during Mesozoic times in association with the opening of the Central Atlantic and the Alpine Tethys. Extensional basins formed along the future continental margin and in the Atlas rift system. In Alpine times, this system was inverted to form the High and Middle Atlas fold-and-thrust belts. To provide a quantitative kinematic analysis of the evolution of the rifted margin, we present a crustal section crossing the Atlantic margin in the region of the Doukkala Basin, the Meseta and the Atlas system. We construct a post-rift upper crustal section compensating for Tertiary to present vertical movements and horizontal deformations, and we conduct numerical modeling to test quantitative relations between amounts and distribution of thinning and related vertical movements. Rifting along the transect began in the Late Triassic and ended with the appearance of oceanic crust at 175 Ma. Subsidence, possibly related to crustal thinning, continued in the Atlas rift in the Middle Jurassic. The numerical models confirm that the margin experienced a polyphase rifting history. The lithosphere along the transect preserved some strength throughout rifting with the Effective Elastic Thickness corresponding to an isotherm of 450°C. A mid-crustal level of necking of 15 km characterized the pre-rift lithosphere. **Citation:** Gouiza, M., G. Bertotti, M. Hafid, and S. Cloetingh (2010), Kinematic and thermal evolution of the Moroccan rifted continental margin: Doukkala-High Atlas transect, *Tectonics*, *29*, TC5008, doi:10.1029/2009TC002464.

1. Introduction

[2] In Late Triassic times, or possibly earlier, continental rifting began in the area of the future Central Atlantic leading to the Middle Jurassic appearance of the Atlantic oceanic crust and, thereby, to the formation of passive continental margins along eastern North America and NW Africa (Figure 1) [*Bird et al.*, 2007]. Extensional basins formed during rifting and are found all along the two conjugate margins, both onshore and offshore (Figure 1) [*Withjack et al.*, 1998]. These basins are typically filled by fluvial-deltaic and lacustrine mudstones to conglomerates [*Manspeizer*, 1988; *Olsen*, 1997] with local intercalations of limestones and evaporites [*Van Houten*, 1977].

[3] The Central Atlantic margin of NW Africa extends from Morocco to Guinea [e.g., *Davison*, 2005] and is characterized by sedimentary basins with a largely similar first-order evolution. The typical sedimentary succession of offshore basins is composed of Triassic red beds, Lower Liassic evaporites (as far south as Senegal), Jurassic to Lower Cretaceous carbonate platforms passing ocean-ward to deep water equivalents, and generally fine-grained marine clastic deposits in the Cretaceous and Tertiary [*Davison*, 2005]. Onshore successions are more incomplete and generally characterized by shallow water deposition.

[4] In Morocco [*Le Roy and Piqué*, 2001; *Davison*, 2005], Late Triassic to Liassic stretching caused the formation of extensional structures in the future passive continental margin (including the Doukkala basin to the North, the Essaouira, Souss, Tarfaya, Layoune and Dakhla basins to the South). To the E of these basins, an ENE-WSW trending rift system developed which was inverted in Tertiary times giving rise to the High and Middle Atlas fold-and-thrust belt (Figure 2). In NW Morocco, the region traversed by our regional transect, the two domains are partially separated by the Moroccan Meseta, an area which, according to conventional knowledge experienced little vertical movements after the Hercynian orogeny [e.g., *Michard*, 1976; *Piqué et al.*, 1980]. Further to the south, more than 100 km away from the transect, the Atlas inverted rift joins the roughly N-S trending Atlantic margin.

[5] Traditionally, Atlas rifting has been related to the opening of the Alpine Tethys Ocean rather than of the Central Atlantic [*Laville and Piqué*, 1991; *Charrière*, 1996]. As extension in the two domains is (partly) coeval, our analysis will include both systems irrespective of their paleogeographic definition (Central Atlantic versus Alpine Tethys).

[6] While a substantial body of literature is available on the sedimentary successions accumulated in the Moroccan Atlantic margin and in the Atlas, only a few tectonic reconstructions exist [*Le Roy*, 1997; *Favre and Stampfli*, 1992], and limited comprehensive studies on the syn- and post-rift evolution of the margin have been presented [*Hafid*, 2000; *Hafid et al.*, 2006]. The core of our study is the quantitative reconstruction of extension and vertical movements along a section crossing the Atlantic rifted margin and the Atlas rift (Figures 1 and 2). The inclusion of

[1]Department of Tectonics and Structural Geology, VU University, Amsterdam, Netherlands.
[2]Netherlands Research Centre for Integrated Solid Earth Sciences, Amsterdam, Netherlands.
[3]Department of Geotechnology, Delft University of Technology, Delft, Netherlands.
[4]Département de Géologie, Faculté des Sciencces, L'Université Ibn Tofail, Kenitra, Morocco.

0278-7407/10/2009TC002464

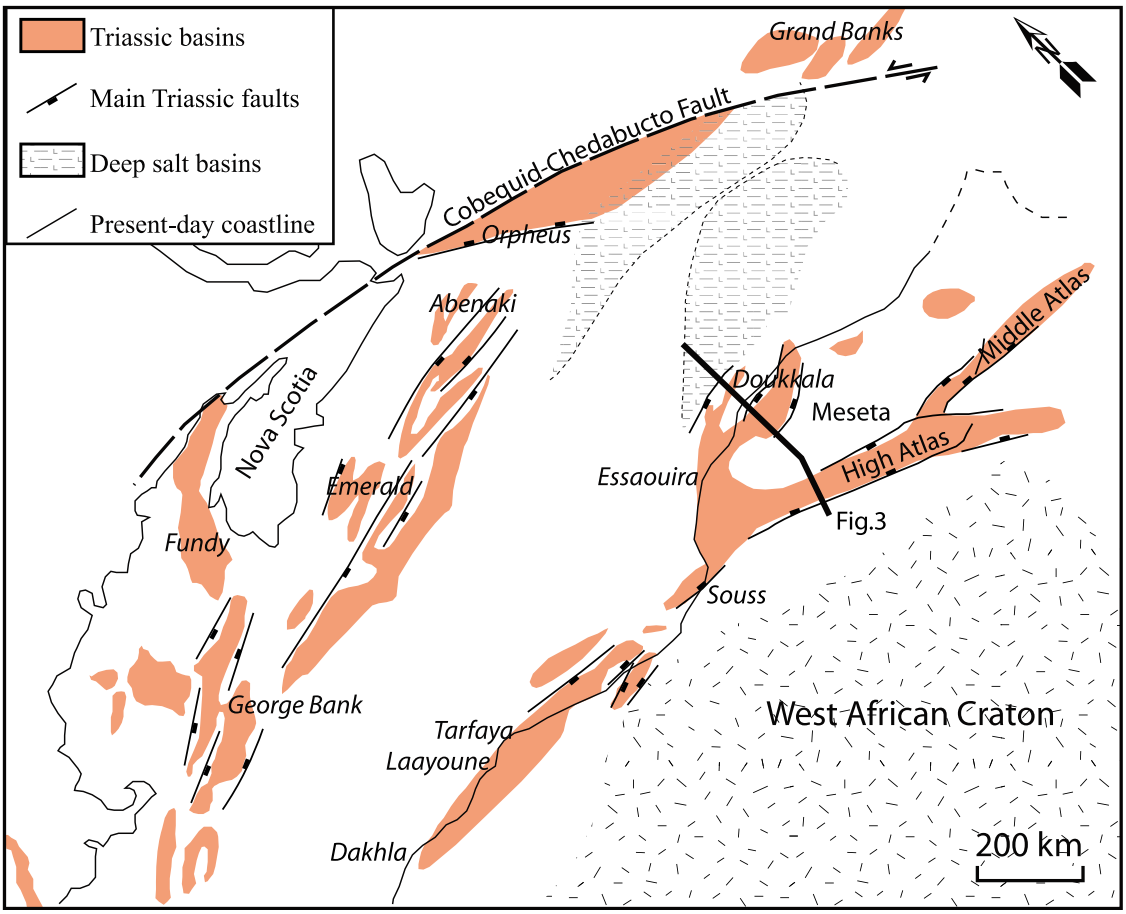

Figure 1. Map of the Central Atlantic domain, showing the correlation between the main Triassic basins just prior to continental break-up (modified after *Le Roy and Piqué* [2001] and *Davison* [2005] with permission from Elsevier). The bold line across NW Morocco indicates the trace of the Doukkala-High Atlas transect (Figure 3).

the Atlas rift in our analysis, obviously introducing some elements of uncertainties, is based on the notion that the two extensional systems operated roughly coeval.

[7] Our paper aims at (1) determining the kinematics of extension affecting the Moroccan rifted margin as a whole and its different domains including for the first time the Meseta and the Atlasic trough; (2) estimating the vertical movements which took place during and following rifting; and (3) testing quantitative relations between lithospheric (crustal and subcrustal) thinning and vertical movements using numerical models. Among others, we investigate processes controlling the well-known and enigmatic Middle Jurassic subsidence documented in the High Atlas.

[8] To this purpose, we first construct a geological cross-section stretching from the Atlantic oceanic crust to the southern reaches of the High Atlas based on field observations, seismic and well data. We then filter out Tertiary to Present deformations and movements to obtain a Late Cretaceous (65 Ma) section through the Moroccan rifted continental margin. We name this the Doukkala-High Atlas transect. We use this profile to determine the kinematics of extension, syn- and post-rift vertical movements as the base for the numerical modeling. We incorporate the diachronous character of the rift by defining rifting stages with different sets of thinning factors. Subsequently, the regional implications of our results are discussed.

2. Geological Setting

[9] The tectonic evolution of Morocco following the Hercynian orogeny is marked by two major stages [e.g., *Michard et al.*, 2008]: (1) A phase of probably Late Triassic to Early Jurassic continental rifting which eventually led to the opening of the Central Atlantic ocean and to the formation of the NW Africa passive continental margin, and (2) Late Cretaceous to Recent continent-continent convergence between Africa and Iberia/Europe which caused the development of fold-and-thrust belts in the Rif [e.g., *Frizon de Lamotte et al.*, 1991] and Atlas Mountains [e.g., *Frizon de Lamotte et al.*, 2000; *Teixell et al.*, 2003]. This second contractional phase with associated thermal events is not relevant for our study and will not be further discussed.

[10] The quantitative reconstruction of the history of rifting requires a definition of the onset and duration of rifting which resulted in the formation of Central Atlantic oceanic crust. We adopt a regional definition of rifting which starts

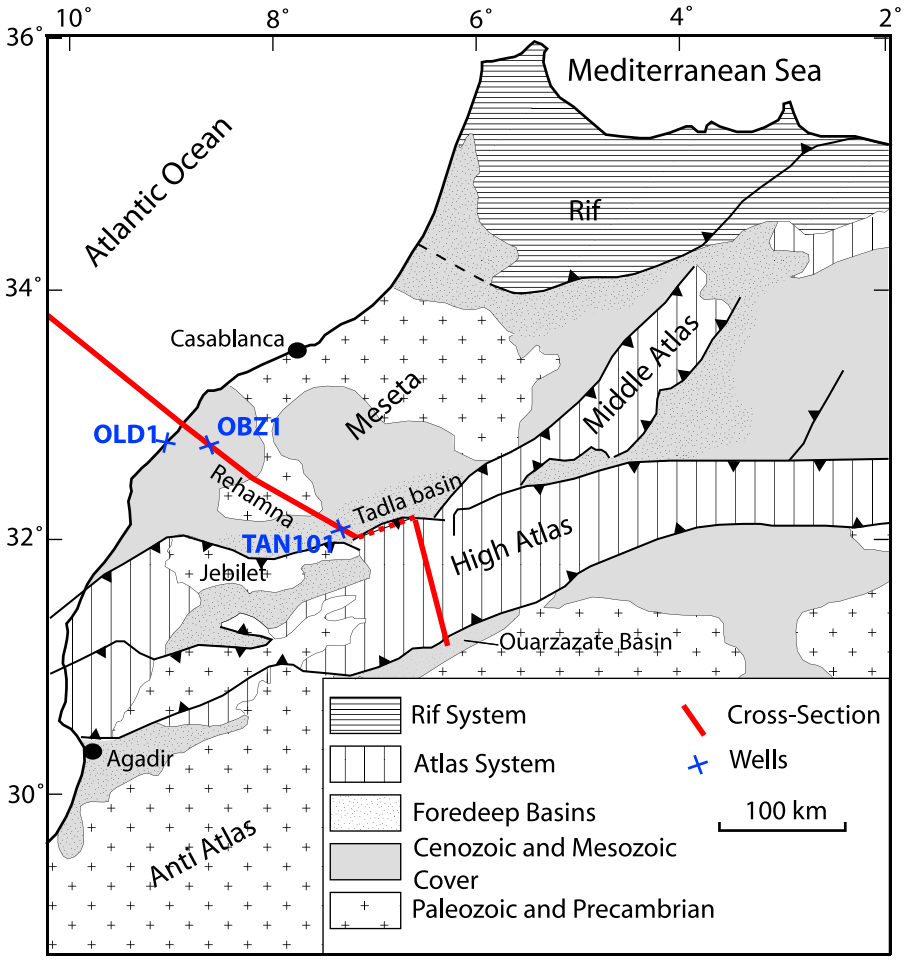

Figure 2. Schematic geological map showing the structural provinces of Northern Morocco (modified after *Hafid et al.* [2006]). The line indicates the position of the Doukkala-High Atlas transect; the crosses indicate the position of the industrial boreholes OLD1, OBZ1 and TAN101.

with the onset of extension leading to the crustal separation and ends with the first appearance of oceanic crust. Obviously, such a regional definition of the rifting period does not imply that extensional basins along the margin developed at the same time. Actually, migration of the site of extension is well known to occur as a consequence of syn-rift lithospheric cooling and strengthening [e.g., *Bertotti et al.*, 1997; *Van Wijk and Cloetingh*, 2002].

[11] The age of the onset of extension leading to the formation of the Moroccan continental margin is poorly constrained due to the presence of Late Permian and Early Triassic basins in the western Atlas and elsewhere [*Hafid*, 2000; *Withjack et al.*, 2010]. Based on regional knowledge from the Central Atlantic margins, we assume that these basins did not form in association with the final break-up of Pangea and, therefore, will not be included in our discussion. In addition, pre-Late Triassic basins are located several tens of kilometers away from our section and, therefore, have little impact on the performed modeling work and the reached conclusions.

[12] Late Triassic to Early Jurassic rifting caused the formation of numerous extensional basins presently found in the Moroccan offshore domain, the continental shelf/coastal plain areas and, to the E of the Moroccan Meseta, in the inverted Atlas system (Figure 2).

[13] The age of the onset of extension in the western parts of the Atlas rift (High Atlas of Marrakech) is well dated as Anisian (~240 Ma) by *El Arabi et al.* [2006] and becomes unclear toward the central parts, where the first syn-rift sediments are assumed to be Carnian (~228 Ma) [*Beauchamp*, 1988; *Laville et al.*, 2004]. However, west of the Atlas in the Doukkala basin, the first extensional episodes are younger and are dated as Rhaetian (~210Ma) [*Medina*, 1995; *Le Roy*, 1997; *Le Roy and Piqué*, 2001]. The infill of the extensional basins is typically formed by Triassic red beds [*Echarfaoui*, 2003; *Hafid*, 2006], followed by uppermost Triassic basalts of the Central Atlantic Magmatic Province (CAMP) (200 ± 1 Ma [*Verati et al.*, 2007]) and Lower Jurassic evaporites. Normal faulting ended in Hettangian/Sinemurian times (~196Ma) in the extensional basins presently found in the coastal to deep-water domains [*Le Roy*, 1997]. The end of extension is less well-constrained in the Atlas rift where pronounced subsidence persisted until Middle Jurassic times possibly controlled by transtensional tectonics [*Laville et al.*, 2004].

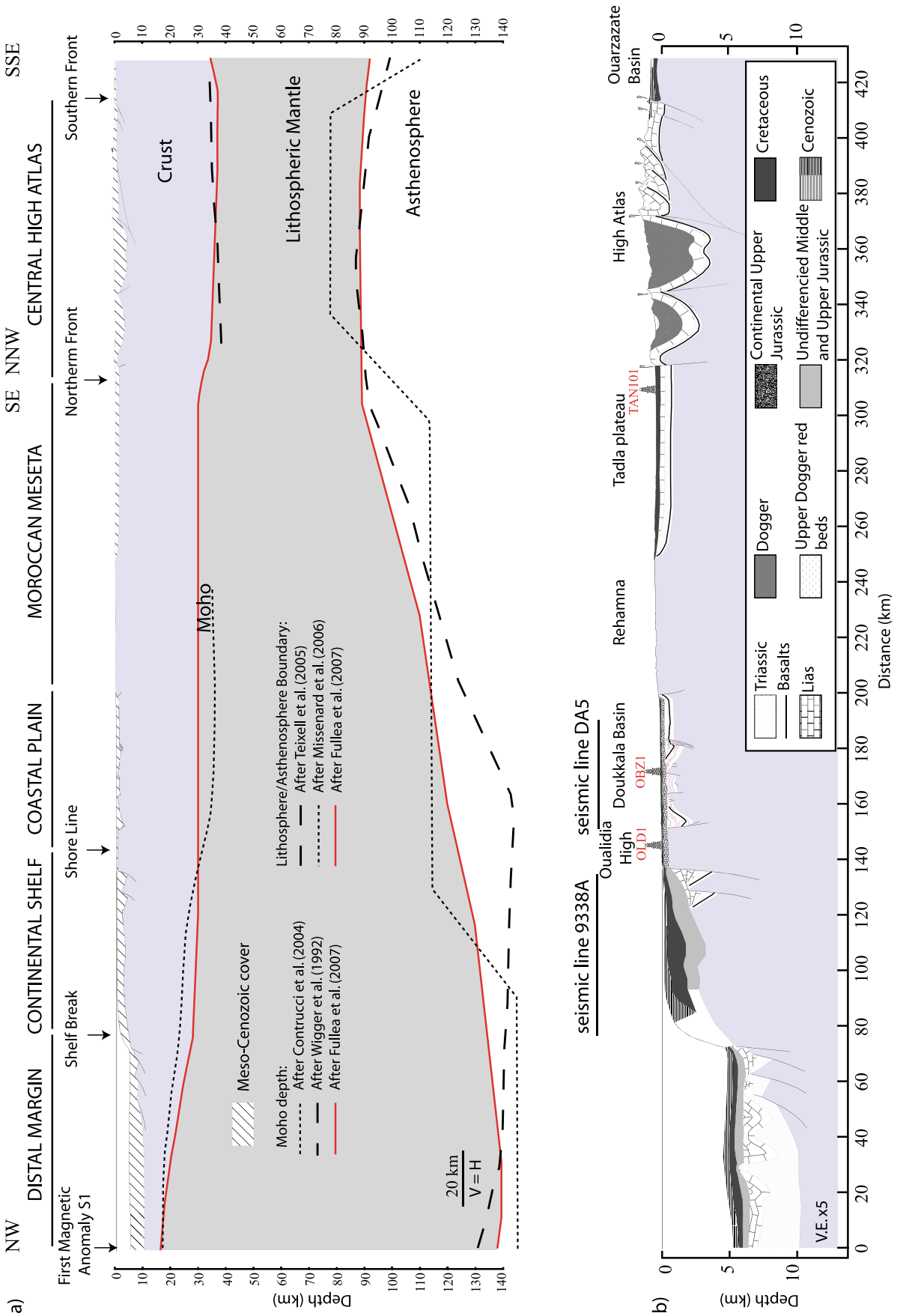
a)
NW
SE
NNW
SSE
DISTAL MARGIN
CONTINENTAL SHELF
COASTAL PLAIN
MOROCCAN MESETA
CENTRAL HIGH ATLAS
First Magnetic Anomaly S1
Shelf Break
Shore Line
Northern Front
Southern Front
Crust
Moho
Lithospheric Mantle
Asthenosphere
Meso-Cenozoic cover
Moho depth:
After Contrucci et al. (2004)
After Wigger et al. (1992)
After Fullea et al. (2007)
Lithosphere/Asthenosphere Boundary:
After Teixell et al. (2005)
After Missenard et al. (2006)
After Fullea et al. (2007)
20 km
V = H
Depth (km)
b)
seismic line 9338A
seismic line DA5
Oualidia High
Doukkala Basin
Rehamna
Tadla plateau
High Atlas
Ouarzazate Basin
OLD1
OBZ1
TAN101
Triassic
Basalts
Lias
Dogger
Upper Dogger red beds
Continental Upper Jurassic
Undifferencied Middle and Upper Jurassic
Cretaceous
Cenozoic
V.E.x5
Depth (km)
Distance (km)

Figure 3

[14] The age of the oldest oceanic crust and, thereby, of the syn-rift to post-rift transition is debated and hinges on the interpretation of the age of the East Coast Magnetic Anomaly (ECMA) and its possible correlative in NW Africa (see *Sahabi et al.* [2004] for a detailed discussion of the problem). According to most authors, [e.g., *Klitgord and Schouten*, 1986; *Davison*, 2005] the ECMA is 175 Ma old, which would then correspond to the age of formation of the first oceanic crust. This would imply a time gap between the cessation of normal faulting and the appearance of oceanic crust which might be explained envisaging the 196–175 Ma as the time interval during which lithospheric mantle was exhumed from underneath its crustal lid [e.g., *Péron-Pinvidic and Manatschal*, 2009]. Alternatively, the ECMA could be as old as 195 Ma thereby making significantly older the onset of ocean spreading [*Sahabi et al.*, 2004] and eliminating the time gap between the end of extension and the creation of oceanic crust. Following the appearance of oceanic crust, the system entered the passive margin stage with primarily thermal subsidence until the Late Cretaceous-Early Tertiary when its evolution became affected by the first stages of contraction related to Africa-Europe convergence.

3. Present-Day Section

3.1. Data and Methods

[15] We have constructed a 450-km-long section running roughly in a NW-SE direction from the continent-ocean transition in the NW to the Ouarzazate basin (between the Anti Atlas and High Atlas) in the SE (Figure 2). The chosen NW-SE direction is more or less parallel to the opening direction of the Central Atlantic Ocean and of the Atlas rift [*Ait-Brahim et al.*, 2002]. The section crosses from NW to SE the offshore margin, the coastal plain, the Meseta domain inclusive of the Rehamna high and Tadla plain, and finally passes the Central High Atlas (Figure 2).

[16] Regional estimates of crustal thicknesses (Figure 3a) have been proposed by *Fullea et al.* [2007] on the basis of the analysis of regional elevation, geoid anomaly and thermal structure. Other crustal thickness data in parts of the section are derived from seismic records from the offshore part of the margin (wide-angle and reflection survey SISMAR Profile-4 [*Contrucci et al.*, 2004]) and from the Atlas region [*Giese and Jacobshagen*, 1992]. Additional information in the High Atlas is provided by electrical resistivity modeling [*Schwarz et al.*, 1992], seismic refraction data [*Wigger et al.*, 1992] and gravity modeling [*Ayarza et al.*, 2005]. On the whole, the Moho position and crustal thicknesses are relatively well constrained.

[17] The depth of the lithosphere-asthenosphere transition (Figure 3a) is estimated on the basis of gravity modeling and geoid analysis [*Fullea et al.*, 2007] and on the interpretation of the few scattered heat flow measurements available [*Rimi*, 1999]. On the whole, the quality of these estimates is unsatisfactory and the geometry of the basis of the lithosphere along the transect is poorly constrained.

[18] We derive upper crustal geometries (Figure 3b) in the distal domain from interpretations by *Le Roy* [1997]. The available data (e.g., SISMAR profile [*Contrucci et al.*, 2004]) only gives information on the thickness of the sedimentary succession, and the stratigraphic architecture in this part of the margin remains poorly constrained. Some constraints on lithologies are provided by boreholes DSDP 370/416 [*Price*, 1981]. For the continental shelf and the coastal domain we have used seismic profiles 9338A and DA5, respectively, which have been previously interpreted by *Le Roy* [1997] and *Echarfaoui* [2003]. Three wells (TAN101, OBZ1 and OLD1) have been drilled along the section or on its continuation (Figure 2) constraining the stratigraphic and sedimentological characterization of the sediments. The time-to-depth conversion of these seismic lines was performed manually using the interval velocities reported on the lines integrated with estimates from seismic cuttings and regional considerations. For the Meseta and the High Atlas the section relies on the excellent geological maps of Morocco and on the numerous published sections [*Laville et al.*, 2004; *Teixell et al.*, 2003; *Arboleya et al.*, 2004; *El Harfi et al.*, 2006].

3.2. Lithosphere and Crust

[19] In the westernmost part of the section (Figure 3a), close to the continent-ocean transition, estimates by different authors suggest Moho depths of ~17 km. According to *Fullea et al.* [2007], the Moho deepens toward the SE reaching a depth of ~29 km underneath the shelf break and then remaining at roughly constant depth until the northern front of the Atlas where it deepens to ~38 km. Interpretations from *Contrucci et al.* [2004] are different and envisage a Moho deepening toward the SE more gently than *Fullea et al.* [2007] but reaching higher values of ~33 km already underneath the coastal plain. In correspondence with the High Atlas, Moho depths estimated by *Wigger et al.* [1992] roughly coincide with those of *Fullea et al.* [2007]. South of the High Atlas, the Moho remains deep and only gently shallows S of the southern front.

[20] Interpretations of the position of the lithosphere-asthenosphere boundary (LAB) (Figure 3) present large variability. On the whole, the different authors agree in estimating the depth of the LAB at 130–145 km at the NW end of the transect and at much shallower depths between 78 and 90 km underneath the High Atlas belt. The geometry of transition between the two areas is, on the contrary, poorly defined. According to *Fullea et al.* [2007], the LAB gently and progressively shallows from the NW to the High Atlas subsurface. A more abrupt transition is proposed by *Teixell et al.* [2005] and *Missenard et al.* [2006] according to whom the LAB only begins to shallow underneath the Meseta.

Figure 3. Present-day cross-section of the Doukkala-High Atlas continental margin of Morocco. (a) Lithospheric section showing different interpretations of the Moho depth and the lithosphere-asthenosphere boundary (LAB). (b) Upper crustal section showing the different basins and their stratigraphic architecture. The position of wells and seismic data used for this study is indicated.

3.3. Upper Crust

[21] In the upper crust of the present-day section (Figure 3b) we distinguish five main domains from NW to SE: the distal margin, the continental shelf, the coastal area, the Meseta and the High Atlas.

[22] The distal margin, with water depths in excess of 4000 m, shows a less than 5 km thick sedimentary succession with less than 1 km of Cretaceous to Recent mainly fine-grained siliciclastic deposits, 1.2–2 km of Jurassic limestone and an up to 3 km thick succession of Triassic evaporites. These form large, generally symmetric diapirs probably developed in mid-Tertiary times [*Tari et al.*, 2007]. Mainly NW-dipping normal faults have been inferred from the seismic line, which dissect Triassic and older rocks and are sealed by Liassic sediments. At about 80 km from the NW end of the section, water depths rapidly decrease in correspondence with the continental slope which is only 20–30 km wide.

[23] The continental shelf-coastal plain area is a 100–120 km wide, geologically fairly homogeneous region. Its upper part is characterized by a Jurassic to Quaternary sedimentary wedge, ~3 km thick at the shelf break, thinning toward the SE and eventually terminating against the Meseta basement. The wedge is basically undisturbed and unconformably overlies the acoustic basement in the NW and a complex domain composed of two extensional systems separated by the Oualidia high in the SE (Figure 3b). The northwestern extensional system is characterized by two main NW-dipping faults. The domain SE of the Oualidia high, known as Doukkala basin, is a Triassic symmetric graben inverted and partly eroded before the Late Jurassic (see below) [*Hafid et al.*, 2008]. At their SE termination against the Meseta block, Triassic layers are folded probably in association with a SE dipping reverse fault (Figure 3b).

[24] The Meseta domain is the part of the section between the Doukkala basin and the northern Atlas front. The Hercynian metamorphic basement [*Hoepffner et al.*, 2005] is exposed in the NW part of the domain (Rehamna) and deepens toward the SE allowing for the preservation of sediments forming a sedimentary wedge (Tadla basin) which reaches its maximum thickness of ~2 km against the High Atlas boundary faults [*Teixell et al.*, 2003; *Hafid et al.*, 2006]. The wedge is composed of an upper, generally undisturbed part of Upper Cretaceous sediments unconformably overlying a Triassic to Liassic succession with a large stratigraphic gap.

[25] The SE-most part of the transect is formed by the central portion of the High Atlas, a well-known fold-and-thrust belt stretching from the Atlantic coast to Tunisia [*Teixell et al.*, 2003; *Frizon de Lamotte et al.*, 2000, 2008]. In the area traversed by the profile, the Atlas range is essentially made up of Mesozoic sediments partly detached from their Hercynian substratum. The succession is typically composed of syn-extensional Triassic detritic red beds and tholeiitic basalts, Lower Liassic carbonates [*Laville et al.*, 1995] and thick series of marls, calciturbidites and limestones accumulated in Dogger times [*Du Dresnay*, 1987; *Warme*, 1988]. Upper Dogger red beds, preserved only in some synclines, terminate the Jurassic succession, indicative of a generalized regression [*Choubert and Faure-Muret*, 1962]. The Malm is generally considered as a time of non-deposition and since the paleontological record is poor, the extent of the gap is debated [*Charrière et al.*, 2005]. Lower Cretaceous rocks are rarely preserved and made up of fluvial deposits overlain by Upper Cretaceous shallow water limestones and phosphatic layers. Angular unconformities are sometimes found at the basis of the Lower Cretaceous and have been associated with transpressional deformation [*Laville and Piqué*, 1992]. Cenozoic rocks are preserved in the small and discontinuous foreland basins flanking the mountain belt such as the Ouarzazate basin and are generally composed of Paleocene to Eocene shallow marine sediments overlain by continental and lacustrine deposits [*El Harfi et al.*, 2001].

[26] Deformation in the High Atlas (Figure 3b) is typically accommodated by thrusts and reverse faults vergent toward the northern and southern forelands. Thrusts are thick-skinned in the northern front (Figure 3b), with tectonic shortening being accommodated by the inversion of Triassic faults, and thin-skinned in the south where contraction occurred along gently dipping faults with a detachment level in Upper Triassic and Upper Cretaceous evaporite and clay beds [*Benammi et al.*, 2001; *Teixell et al.*, 2003; *El Harfi et al.*, 2006].

4. Doukkala-High Atlas Rifted Continental Margin in the Late Cretaceous

[27] To obtain a post-rift, pre-orogenic upper crustal section across the entire NW Moroccan rifted margin from the Atlantic Ocean to the southern stretches of the High Atlas we have filtered out Tertiary to Present horizontal deformations and vertical movements from the section of Figure 3b.

4.1. Methods and Uncertainties

[28] To compensate for Tertiary to Present vertical movements, we have used the 2DMove® software. As no consistent information was available on porosity distributions, we did not implement sediment decompaction.

[29] In the distal part of the margin, we have removed Tertiary to Recent sediments and smoothed out possible diapirs [*Tari et al.*, 2007]. In the absence of data constraining the paleowater depths, we have used a linear interpolation between the 0 m water depth at the end of the Liassic and the present-day bathymetry. With this approach we obtained a water depth of ~2 km at 65 Ma.

[30] In the continental shelf/coastal plain domain, not many modifications to the present section were needed, as Tertiary to present sediments are less than 1 km thick and undeformed.

[31] The vertical position of the top of the Meseta block in the Late Cretaceous is well constrained by the presence of Upper Cretaceous shallow marine sediments observed in areas immediately to the N of the transect of interest. The thickness of these sediments is based on information from the adjacent Settat region, where coeval deposits are pre-

served in the SE part of the Doukkala Basin and in the Tadla basin. We use thickness data from regions contiguous to the transect based on the assumption that (part of) the deformation affecting the NW and SE margins of the Rehamna basement block is of Tertiary age. In the Meseta region, the base of the Upper Cretaceous is a regional unconformity, which covers scattered remnants of the Upper Triassic (in the N and E) and a somewhat more continuous succession of red beds possibly of Late Jurassic to Early Cretaceous age in the W.

[32] The High Atlas is the part of the section which experienced the most significant post-Mesozoic horizontal shortening. Our restoration to Late Cretaceous times is based on bed lengths, essentially from competent Lower Liassic strata. Our reconstruction is accurate in the NW part of the section where high angle faults dominate and do not alter significantly the original length of syn-rift layers [*Frizon de Lamotte et al.*, 2004; *El Harfi et al.*, 2006]. The restored section in the S is less reliable as shortening is mainly accommodated by low-angle faults and parts of the Upper Triassic-Lower Liassic beds might have been eroded. The thickness of Cretaceous layer was extrapolated by surrounding areas (i.e., Tadla to the W and Ouarzazate to the E). Our restoration yields a total shortening of 32 km (i.e., 17%) compatible with findings by previous authors [*Beauchamp et al.*, 1999; *Teixell et al.*, 2003; *Frizon de Lamotte et al.*, 2008]. As the largest majority of normal faults were inverted in Tertiary times, the reconstruction of the geometry of the rift basin is mainly based on the recognition of abrupt thickness changes in coeval sedimentary packages presently preserved in adjacent fault blocks.

4.2. Post-Rift

[33] Post-rift sediments are found over the entire section, from the Central Atlantic to the southern reaches of the High Atlas (Figure 4). The most continuous and characteristic post-rift interval is the Upper Cretaceous. Over most of the section, with the exception of the distal margin, it is represented by marly carbonates deposited in shallow water settings. In the Atlas region, the Cretaceous has a thickness of few hundred meters, which decreases to 150 m in the Tadla plain and increases gradually to the W over the continental shelf domain where it is ~1500 m thick. NW of the shelf break (Figure 4) the platform carbonates pass to deep water, with more shaly equivalents.

[34] The thickness and facies continuity of Upper Cretaceous sediments over most of the section is contrasting with the large variability of the underlying sediment succession where important, laterally changing stratigraphic gaps are present (Figure 5). In the deep margin, the Mesozoic succession is generally continuous. The Lower Cretaceous part of the section (Hauterivian-Valanginian) was drilled at DSDP sites 370 and 416 and is composed of coarser-than-normal sands with carbonate clasts at the bottom and terrigenous elements in the upper part [*Price*, 1981].

[35] A stratigraphic gap appears in the continental shelf area where Middle Jurassic sediments lie directly in contact with the acoustic basement (Figures 4 and 5). With the exception of the extensional basins NW of the Oualidia high, the stratigraphic gap increases to the SE part of the Meseta (Rehamna). In the subsurface of the Tadla plain the Upper Jurassic to Lower Cretaceous is missing and Upper Cretaceous beds are in direct contact with the Liassic. Entering the High Atlas rift, the succession becomes thicker and relatively more complete. Upper Cretaceous carbonates overly poorly dated red beds typically deposited in fluvial settings generically considered as Lower Cretaceous possibly Upper Jurassic; stratigraphic gaps are likely [*Ruellan*, 1985; *Le Roy*, 1997; *Ellouz et al.*, 2003]. Middle Jurassic sediments in the Atlas domain are shallow water carbonates present with remarkable thickness in the axial domain [*Laville et al.*, 2004]. They are absent in the southern reaches of the Central High Atlas.

4.3. Syn-Rift

[36] The syn-rift succession, typically composed of Upper Triassic red beds with CAMP-related volcanic intercalations and Liassic Limestone is found in most parts of the Doukkala-High Atlas transect. Although not directly documented, similar sediments should be present also in the distal part of the margin associated with large masses of evaporites (Central Atlantic Salt Basins) [*Le Roy*, 1997; *Sahabi et al.*, 2004]. Syn-rift sediments show major thickness changes related to coeval extensional basin formation. From NW to SE three main extensional systems are observed in the distal margin, the continental shelf/coastal domain and in the Atlas rift. Geometries in the distal margin along our section are based on the work of *Le Roy* [1997]. Two to three half grabens are identified controlled by W-ward dipping normal faults defining ~10-km-wide eastward tilted blocks. The grabens are sealed by sediments of probable Liassic age. Vertical displacements on these faults are of several hundred meters. The distal margin extensional system is bounded to the SE by a basement high devoid of syn-rift sediments and buried under a thick succession of post-rift deposits.

[37] To the SE of the high, in the continental shelf-coastal plain region, syn-rift sediments are preserved in two extensional systems to the NW and the SE of the Oulidia high where no syn-rift sediments are observed. The region to the W of the high is relatively simple and characterized by a set of W-dipping normal faults defining E-ward tilted fault blocks. Sediments in the half grabens are Upper Triassic red beds intercalated by basalts and several intervals of evaporites, and Lower Liassic carbonates which are organized in E-ward diverging fans. Normal faulting seems to terminate toward the end of the Early Liassic. The region E of the Oualidia high is the Doukkala basin, an inverted structure sealed by Upper Jurassic red beds (Figures 4 and 6a). The extensional Doukkala basin is controlled by a relatively symmetric system of four main normal faults dipping toward the center of the basin. The two normal faults on the NW side of the basin have displacements of ~2000 and ~800 m. The SE side of the basin is dissected by two NW-dipping normal faults with displacements of ~600 and 800 m. Differently from what is observed on the NW side, the southeastern-most fault of the Doukkala basin terminates before the basaltic intercalation which, together with the Upper Triassic, is continuous to the SE and only terminates 17 km further, in correspondence with the faulted margin of the Rehamna

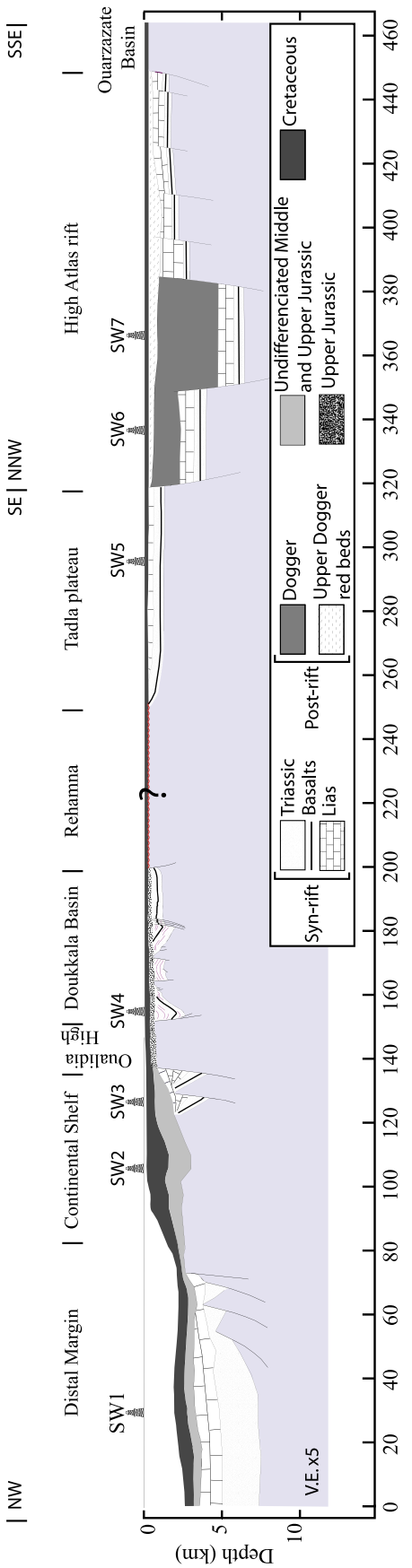

Figure 4. Late Cretaceous (~65 Ma) restoration of Doukkala-High Atlas cross-section.

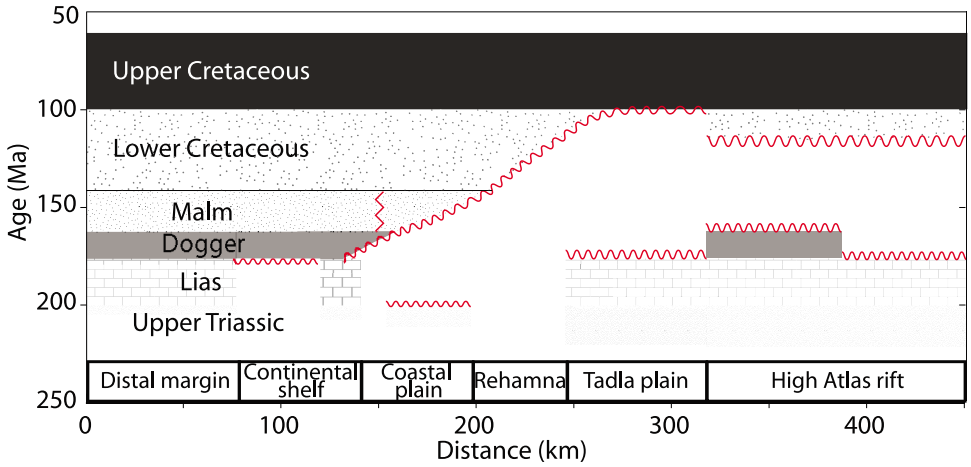

Figure 5. Diagram showing stratigraphic gaps and unconformities underneath the Upper Cretaceous, along the studied section.

basement (Figure 4). Triassic sediments and their substratum are deformed forming an apparent symmetric anticline centered on the depocenter of the extensional basin. The deformed sediments are partly eroded and covered unconformably by subhorizontal layers of probable Upper Jurassic age (Figure 6a).

[38] In the interpretation proposed in the restored section at 65 Ma (Figure 4), syn-rift sediments are absent on the Rehamna basement and only reappear in correspondence with the Tadla basin. Here, Triassic to Liassic sediments exist and thicken to the SE reaching a maximum value of ~1200 m in correspondence with the northern Atlas front.

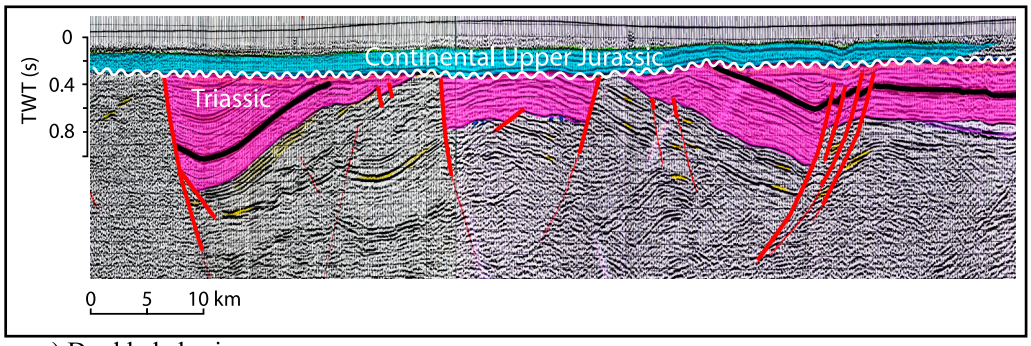

a) Doukkala basin

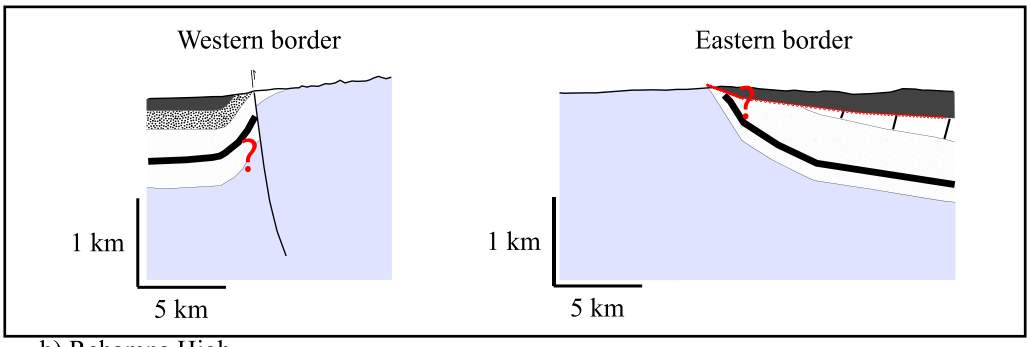

b) Rehamna High

Figure 6. Details of some key-locations in Doukkala-High Atlas transect. (a) Seismic line DA5 throughout Doukkala basin showing the Upper Jurassic red beds unconformably lying above the inverted Upper Triassic half grabens. (b) Western and eastern border of the Rehamna high (after the geologic map of Morocco, scale 1:200,000 [*Gigout*, 1965]).

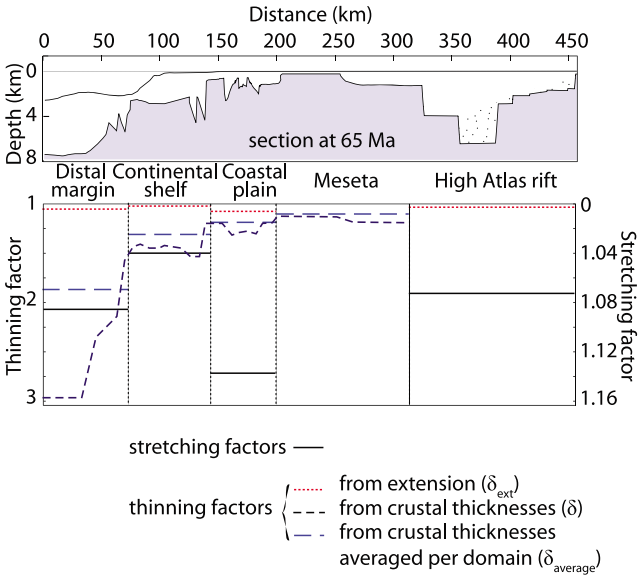

Figure 7. Stretching factors calculated for different domains along the Doukkala-High Atlas transect and crustal thinning factors derived from *Fullea et al.* [2007] (δ) and deduced from the observed amount of extension using mass conservation law (δ_{ext}).

Different from what generally accepted hitherto, we propose that Triassic to Jurassic sediments were probably present also on the Rehamna basement and have been removed during Middle Jurassic to Early Cretaceous exhumation and erosion. This is compatible with (1) the comparable thickness of Triassic sediments in the Tadla basin and in the region NW of the Rehmana basement, (2) recent thermochronologic data [e.g., *Ghorbal et al.*, 2008; *Saddiqi et al.*, 2009], and (3) the geometry of the NW and SE boundaries of the Rehmana basement which document post Jurassic shortening (Figure 6b).

[39] To the SE of the Tadla basin, the Atlas rift presents the largest accumulation of syn-rift sediments in Morocco. The restored cross-section of the High Atlas (Figure 4) shows a rather asymmetric extensional system. Its NW part is controlled by two major faults with displacements of 2.5–3 km. The SE side of the system shows one major fault with an offset of more than 3000 m and a number of smaller features affecting its footwall. Triassic and Liassic sediments thicken gently from the Tadla basin to the center of the Atlas rift to thin again moving away from the rift axis. The distribution of Middle Jurassic sediments is, in contrast, asymmetric as they are absent from the entire footwall of the NW-dipping fault system where Upper Dogger red beds are in direct contact with the Liassic (Figure 4) [*El Harfi et al.*, 2006].

4.4. Pre-Rift

[40] Along most of the section, the Upper Triassic syn-rift deposits are in direct contact with the metamorphic basement and pre-rift sediments are only present in localized, possibly fault-controlled, outcrops. In fact, most of the relief which developed in association with Hercynian exhumation and deformation [*Michard*, 1976] must have been peneplained before Late Triassic time suggesting that the crust had been well equilibrated with basement rocks being close to the Earth's surface.

4.5. Quantitative Description of Syn- and Post-Rift Evolution

4.5.1. Syn-Rift Extension and Crustal Thinning

[41] Based on the fault geometries and sediment thicknesses shown in Figure 4 we have obtained amounts of extension and stretching factors (Lf/Li) for the entire transect and for constitutive segments (Figure 7). The overall amount of extension is low, ~20 km (corresponding to 4.6%) compatible with the generally steep geometry of the normal faults and with the limited number of extensional systems observed. Our estimates are minimum values because of the poorly constrained geometry of normal faults in the distal margin and in the Atlas rift. The total extension is heterogeneously distributed over the distal basin (~6 km), the continental shelf (2.5 km), the coastal plain (4 km) and the Atlas rift (~8 km). Assuming a total duration of rifting of 53 Myr (228–175 Ma) we obtain a strain rate of 8.8×10^{-4} Myr^{-1} for the entire margin. Locally, as in the Doukkala area, higher strain rates of 7.6×10^{-3} Myr^{-1} are obtained as a consequence of strong extension and shorter duration.

[42] Assuming mass (surface in 2-D) conservation, we have translated the stretching factors in the five domains of Figure 7, into thinning factors (δ_{ext}) here defined as the ratio between the initial and the final thickness (Figure 7). These are compared with thinning factors (δ) obtained dividing a conventional initial thickness of 33 km by the present-day crustal thicknesses [*Contrucci et al.*, 2004; *Fullea et al.*, 2007]. Results do not change significantly adopting the other crustal configurations shown in Figure 3a. To facilitate comparison with thinning factors derived from horizontal extension, we present also values ($\delta_{average}$) averaged over each of the five domains indentified along the transect.

[43] Thinning factors obtained by converting extensional strain are lower than those estimated by comparing initial and final thicknesses in the distal margin where imaging is poor and, to a lesser degree, in the Atlas where the present-day thickness is influenced by Tertiary shortening. The difference between the two values is small in the better-constrained areas, i.e., in the continental shelf and in the coastal area.

4.5.2. Vertical Movements During and Following Rifting

[44] To document post-rift subsidence patterns across the Doukkala-High Atlas transect we have constructed subsidence curves for representative localities across the margin (Figure 4) using standard methods [*Allen and Allen*, 2005]. The curves (Figure 8) cover the time frame from the beginning of the syn-rift (Carnian) until the end of the post-rift (Late Cretaceous) when continent-continent convergence, between Africa and Iberia, occurred and initiated the Atlas belt formation.

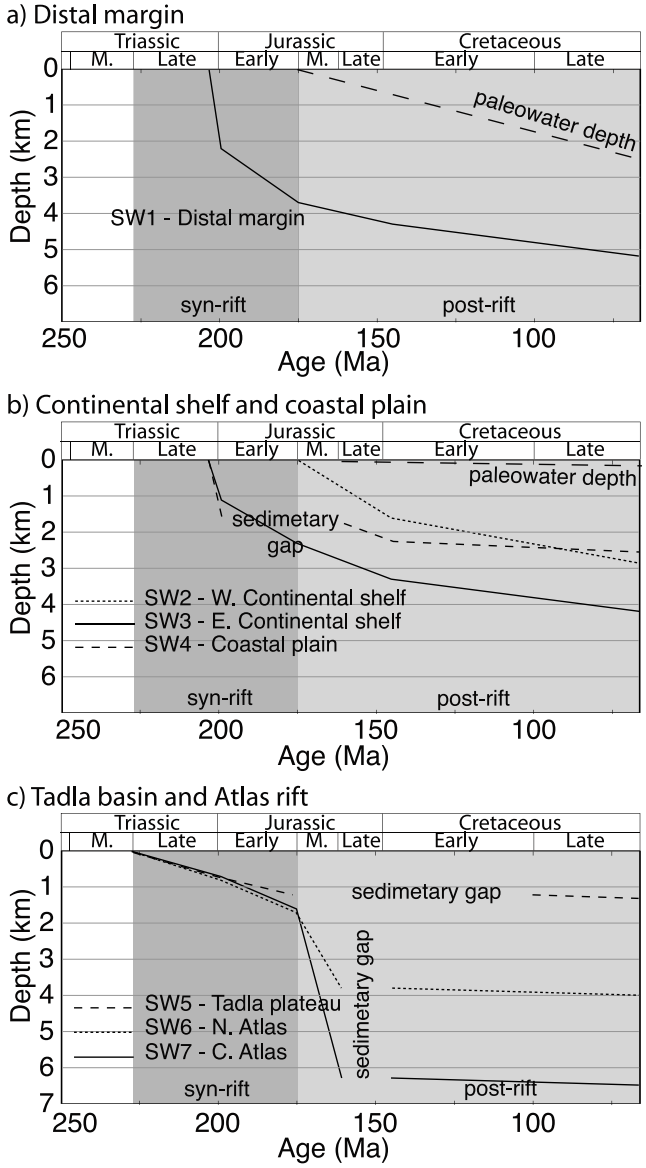

Figure 8. Subsidence curves derived from backstripping different synthetic wells (SW) along the Doukkala-High Atlas margin (see Figure 4 for well location).

[45] The curves have been constructed on the basis of our regional transect (Figure 4). We did not include decompaction in our backstripping analysis. With the exception of the distal margin, paleobathymetries over the main part of the transect are close to 0 m and, therefore, well constrained. The accuracy of subsidence estimates in the distal part of the margin is affected by the poorly known ages of sedimentary successions.

[46] Subsidence in the most distal part of the margin (curve SW1 in Figure 8a) began in the Rhaetian and followed a normal trend with decreasing subsidence rates. Subsidence was only partly compensated by sedimentation and a substantial water column developed.

[47] Curve SW2 (Figure 8b) tracks movements of the basement high at the SE boundary of the distal margin. The high remained stable during the entire rifting stage and began subsiding only in the Middle Jurassic. Subsidence rates decrease from the Cretaceous. Extensional basins to the SE of the basement high (curves SW3 and SW4 in Figure 8b) experienced subsidence beginning in the Rhaetian and continuing then with decreasing rates. While downward movement of the basins to the W of the Oualidia high was continuous at decreasing rates, the subsidence of the Doukkala basin (curve SW4 in Figure 8b) was interrupted by a phase of inversion and erosion, probably in Middle Jurassic times leading to the sedimentary gap reflected in the curve.

[48] The Tadla basin (curve SW5 in Figure 8c) is characterized by Carnian onset of subsidence, very low subsidence rates until the Early Jurassic and a poorly understood sedimentary gap ranging from the middle Jurassic to the Late Cretaceous. Basically no subsidence occurred after this. The subsidence curves of the Atlas rift (curves SW6 and SW7 in Figure 8c) begin at a rate similar to that of the Tadla basin but then accelerate in Middle Jurassic times. Rapid subsidence ended in the Late Jurassic.

5. Two-Dimensional Thermo-Kinematic Modeling of the Doukkala-High Atlas Transect

[49] To quantify relations between extension, thinning and vertical movements during and following rifting, we have performed numerical modeling allowing the regional transect described above. In our 2-D approach we restrict ourselves to the quantification of the response to thinning of structures located along the transect itself.

5.1. Set-Up and Configuration of the Model

[50] The 2-D basin modeling code we use is a finite difference thermo-kinematic model [*Kooi*, 1991; *Kooi et al.*, 1992], which relates crustal and subcrustal thinning to vertical movements. Some of the fundamental features incorporated are finite duration of rifting, non-uniform thinning with depth, multistage rifting, depth of necking, effective elastic thickness, lateral heat flow and flexural behavior of the lithosphere.

[51] In the model, the transect of interest is subdivided into a number of boxes with constant width composed of an upper and a lower part corresponding to the crust and lithospheric mantle. Thinning factors, here defined as the ratio between the initial and the final thickness, for the crustal and for the subcrustal lithosphere are assigned to each box. For each time step, the model calculates the isostatic position of each thinned box. Including paleo-water depth estimates, the model determines the amount of the available accommodation space, fills it with sediments of specified characteristics and iteratively determines the new position of the box (sediment load). Sediment compaction is included in the calculations. We use flexural models, with an effective elastic thickness (EET) described by the position of an isotherm. We also use a depth of necking previously defined as the level in lithosphere that remains horizontal during thinning if effects of sediments and water loading are removed [*Braun and Beaumont*, 1987; *Kooi et al.*, 1992].

Table 1. Different Parameters Used in the Numerical Modeling and Their Respective Values

Parameter	Value
Rifting events[a]	3
Isotherm describing elastic thickness[a]	450°C
Depth of necking[a]	15 km
Initial crustal thickness[a]	33 km
Initial lithospheric thickness[a]	120 km
Coefficient of thermal expansion	0.34×10^{-4} °C^{-1}
Surface temperature	0°C
Asthenospheric temperature	1333°C
Thermal diffusivity	7.8×10^{-7} m^2/s
Mantle density at surface condition	3.33 g.cm^{-3}
Crustal density at surface condition	2.8 g.cm^{-3}
Water density	1.03 g.cm^{-3}
Grain density of the sediments	2.6 g.cm^{-3}
Surface porosity sediment infill	0.5
Characteristic depth constant	0.5
Gravitational acceleration	9.8 m.s^{-2}
Young's modulus	70 GPa
Poisson's ratio	0.25

[a]Parameters with values varying for the different models.

5.2. Model Input

[52] The input of the model is composed of standard values (see Table 1) and parameters specific to the transect of interest. In the numerical model, the Doukkala-High Atlas transect is composed of 64, 7 km-wide boxes (Figure 9). To avoid boundary effects, the region of interest is bounded to the SE by domains which are not thinned but can move vertically as a response to flexural effects. The deep offshore domain is modeled incorporating crustal thinning factors up to 2.8.

[53] For our modeling work we adopt a regional definition of rifting duration which begins in the Carnian (228 Ma) and ends with the appearance of the first oceanic crust at 175 Ma. This duration does not necessarily coincide with the duration of normal faulting in the different parts of the margin. We end our analysis at 65 Ma (Late Cretaceous) which is the age of the regional section in Figure 4 and roughly the age of the transition to more convergence-related deformations.

[54] We adopt an initial crustal thickness of 33 km as suggested by the position close to sea level of the Earth's surface immediately prior to the beginning of rifting and in agreement with present-day values from undeformed parts of Morocco [*Tadili et al.*, 1986; *Wigger et al.*, 1992; *Frizon de Lamotte et al.*, 2004]. Post-rift crustal thickness values and, therefore, thinning factors are derived from the crustal section presented in Figure 3a and are modified only in the Alpine shortened Atlas region in order to obtain an acceptable fit. For the lithosphere, we assume a conventional initial value of 120 km (corresponding to an 87 km thick lithospheric mantle). The thicknesses of the lithosphere at the end of rifting (175 Ma) and at the time span covered by our regional section (65 Ma) are obviously unknown. Thinning factors in the crust of the High Atlas region and in the lithospheric mantle (subcrust) of the entire transect are tuned in order to fit the stratigraphic record and become, therefore, an output of the model.

[55] The history of rifting in Morocco is characterized by significant lateral changes in the amount and timing of thinning. To account for these changes, we subdivided the rifting stage in two phases at 228–200 Ma and 200–175 Ma. When investigating the processes controlling Dogger subsidence in the High Atlas rift, we have added a third phase between 175 and 161 Ma. Thinning factors are constant during each stage but are varied from one to the other, making sure that their cumulative results correspond to the total thinning factors observed. To guide the fine-tuning of the thinning factors, we have considered, beside the necessity of fitting the stratigraphy data, also geological con-

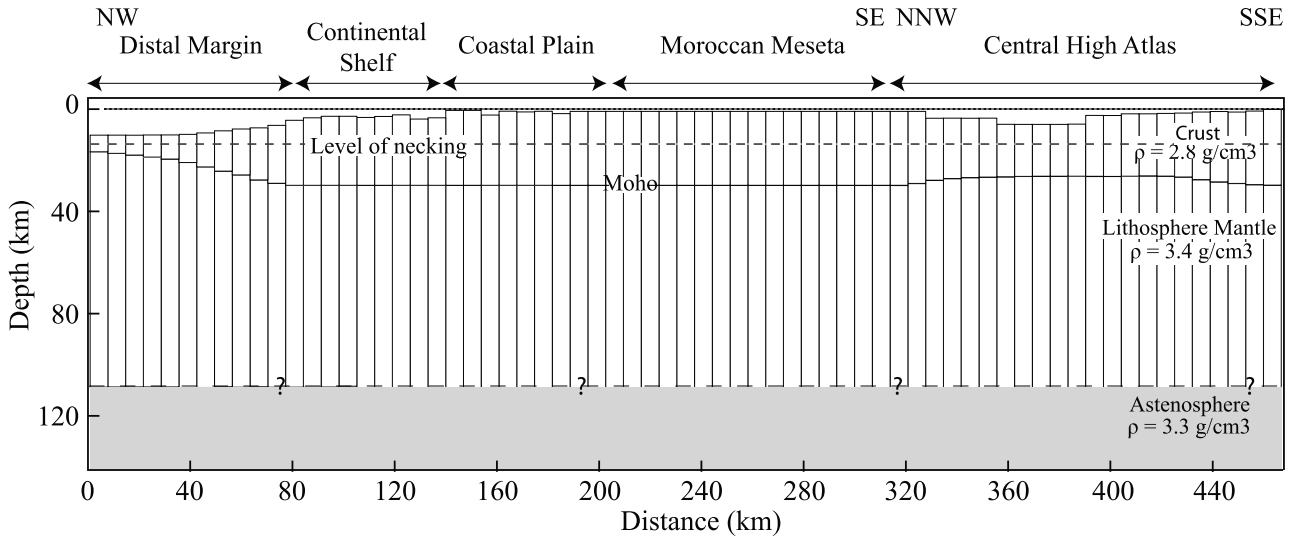

Figure 9. Set-up of the 2-D numerical model of the Doukkala-High Atlas margin at the end of rifting characterized by a level of necking localized in the crust. The initial crustal and lithospheric thicknesses are 33 and 120 km, respectively. Other parameters are given in Table 1.

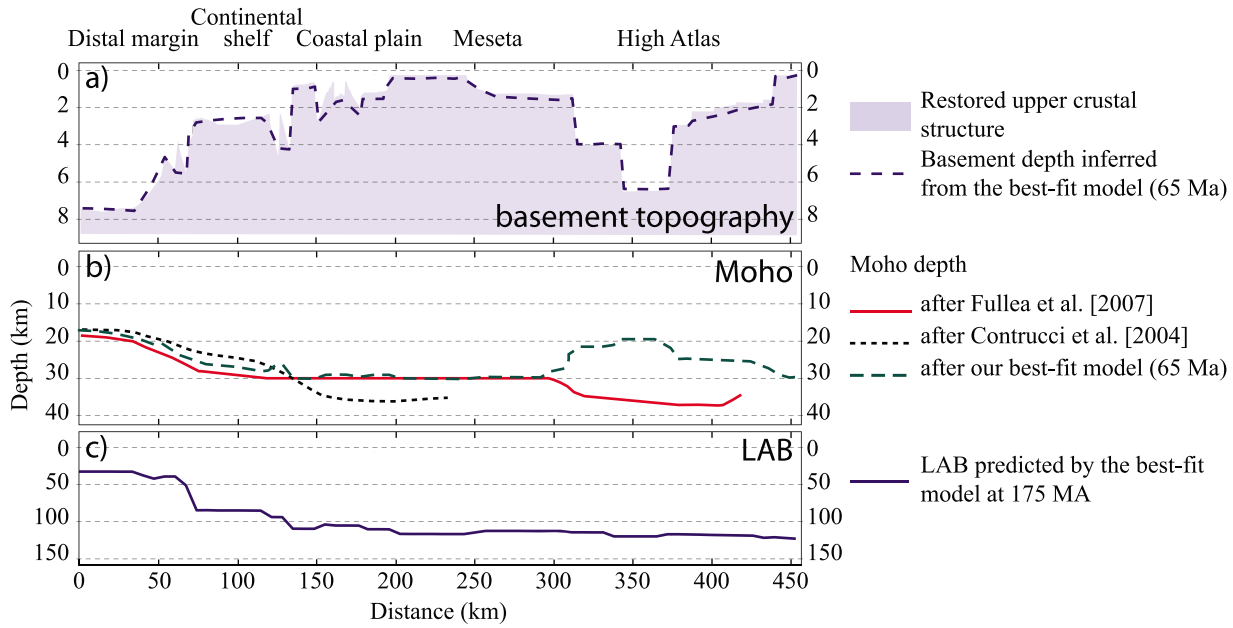

Figure 10. Best fit model results. (a) Basement topography and comparison with the observed Topography. (b) Moho geometry and comparison with other Moho depth estimates. (c) Lithosphere/asthenosphere boundary (LAB).

straints such as, for instance, the age of normal faulting. Thinning factors for the different stages are, therefore, an output of the model. As we could not detect stages of quiescence during rifting, the three stages are not separated by time intervals.

[56] Paleo-water depths of 0 m were adopted at the beginning of rifting over the entire transect including the future distal part of the margin where continental beds and evaporites are suggestive of shallow water conditions. Water depths remained close to 0 m during the syn- and post-rift periods over most of the transect and are, therefore, well constrained. The least well-constrained region is obviously the future distal part of the margin because of its present deep position and of the absence of direct information. For this region we have assumed a linear deepening between 175 Ma (end of rifting stage) and present-day.

5.3. Best Fit Model

5.3.1. Main Features

[57] The model shows a good correspondence of basement topography with respect to the restored section (Figure 10a), except in the center of the coastal plain (Doukkala basin), where the predicted basement is 600 m deeper than the observed one. The too-high position of the observed basement is related to the Jurassic deformation not considered by the model and which caused the inversion of the syn-rift graben and the partial erosion of the Triassic sediments (Figure 6a). The predicted Moho geometry (Figure 10b) is in reasonable agreement with that of *Fullea et al.* [2007], except for the Atlas region where the modeled Moho is up to 15 km shallower than the one predicted by *Fullea et al.* [2007]. We relate this difference to the crustal thickening associated with the Atlas shortening. The predicted lithosphere/asthenosphere boundary (LAB) at the end of rifting (175 Ma) (Figure 10c) is less than 50 km deep in the most distal part of the margin and generally remains constant (100–115 km) from the coastal area to the Atlas rift.

[58] The reproduced stratigraphic architecture is largely consistent throughout the modeled margin (Figure 11). Some discrepancies are found in the southern part of the Atlas rift where the Liassic is ~1 km thicker than in the reconstruction and in the distal margin where the Jurassic deposits are predicted twice as tick as in the restored section.

[59] Subsidence curves extracted from the model compare fairly well with what is observed in the SE part of the section, i.e., in the Tadla region and in the Atlas domain (curve SW5 in Figure 12c, curves SW6 and SW7 in Figure 12d). Curves to the NW of the Rehamna basement show more important misfits. In the poorly constrained distal margin (Figure 12a) the model predicts a subsidence higher than the observed one and an uplift stage not recorded in the data. In the much better constrained continental shelf (Figure 12b) the misfit is less important. In locality SW2, the basement is predicted to remain above sea level contributing to the observed stratigraphic gap. Model-derived Middle Jurassic and younger subsidence is somewhat higher than observed. Predicted subsidence in SW3 is initially similar to what is inferred from the data but then continuous without slow-down until the end of the Early Jurassic when it is interrupted by a stage of upward movement which results from the flexural response to the Middle Jurassic thinning in the adjacent coastal domain. No indications of upward movement are known in the sedimentary

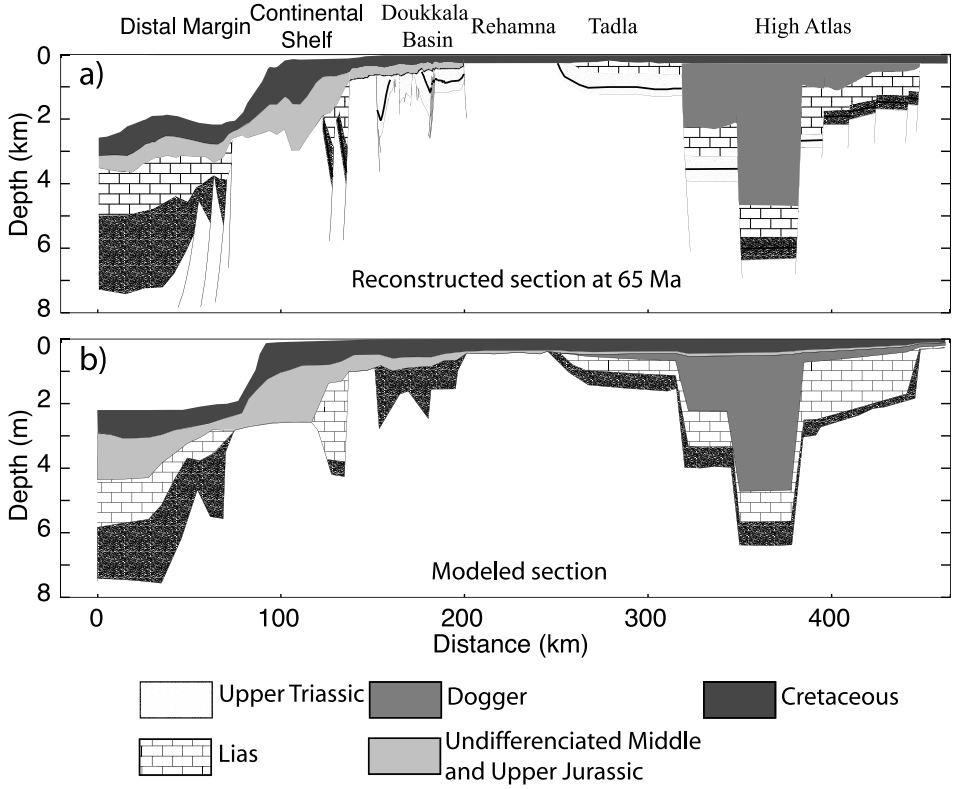

Figure 11. (a) Observed geometries for sediment infill along the Doukkala-High Atlas transect at 65 Ma. (b) Modeled stratigraphy.

record around SW3. Subsidence predicted for synthetic well SW4 (Figure 12c) initially replicates well the data and continues until the end of the Triassic when the top of the pre-rift basement is estimated to have reached depths of ~3 km. A stage of stability followed in the Early Jurassic which turned into uplift in the Middle Jurassic and then to gentle subsidence until the end of the model run. Vertical movements predicted for SW4 in the Early to Middle Jurassic are not incompatible with the stratigraphic column of SW4 which is characterized by a coeval lack of sediments.

5.3.2. Best Fit Parameters

[60] The best fit-model has been obtained with a poly phase history of thinning supporting the assumptions made on the basis of the geological record. The thinning history lasted 67 Ma and was subdivided into three phases, in the Late Triassic (~228–199 Ma), Liassic (~199–175 Ma) and Dogger (175–161 Ma). The model provides insight in the magnitudes of thinning factors through space and time (Figure 13). Crustal thinning in the Late Triassic was strong in the distal part of the margin, absent in the basement high of the continental shelf and had values around 1.1 and 1.2 in the remaining of the section (Figure 13). Subcrustal thinning during this first phase is low (<1.8) and focused mainly in the distal margin and underneath the Doukkala basin region. Crustal thinning became more localized during the second stage and basically was limited to the distal margin (partial factors of ~2.6), part of the continental shelf and the Tadla-Atlas region (partial factors of ~1.5). Subcrustal thinning was basically localized in the most distal part of the margin in association with the imminent rupture of the continental crust but affected also the continental shelf which had previously escaped thinning and had remained therefore at shallow levels. Crustal thinning is predicted to have taken place during the third stage in the continental shelf and, more importantly, in the Atlas region. The model indicates that no subcrustal thinning is required during this stage.

[61] We obtain our best fit model adopting a temperature-dependent effective elastic thickness (EET) defined by the position of the 450°C isotherm (corresponding to a thickness of 40.5 km, before the onset of thinning). The model also predicts an intermediate necking depth of 15 km.

5.4. Sensitivity Analysis

5.4.1. Duration of Rifting and Rifting Events

[62] The best fit model assumes that thinning started at 228 Ma and ended at 175 Ma along the entire transect with the exception of parts of the continental margin and of the Atlas domain where it continued until 161 Ma. At first notice, this appears to be geologically controversial because it implies thinning persisting after the appearance of oceanic crust in the Central Atlantic. In a modeling perspective, the necessity of Dogger crustal thinning is fairly robust and a simulation with thinning ending at 175 Ma along the entire transect produces in the Atlas region a syn-rift stratigraphy

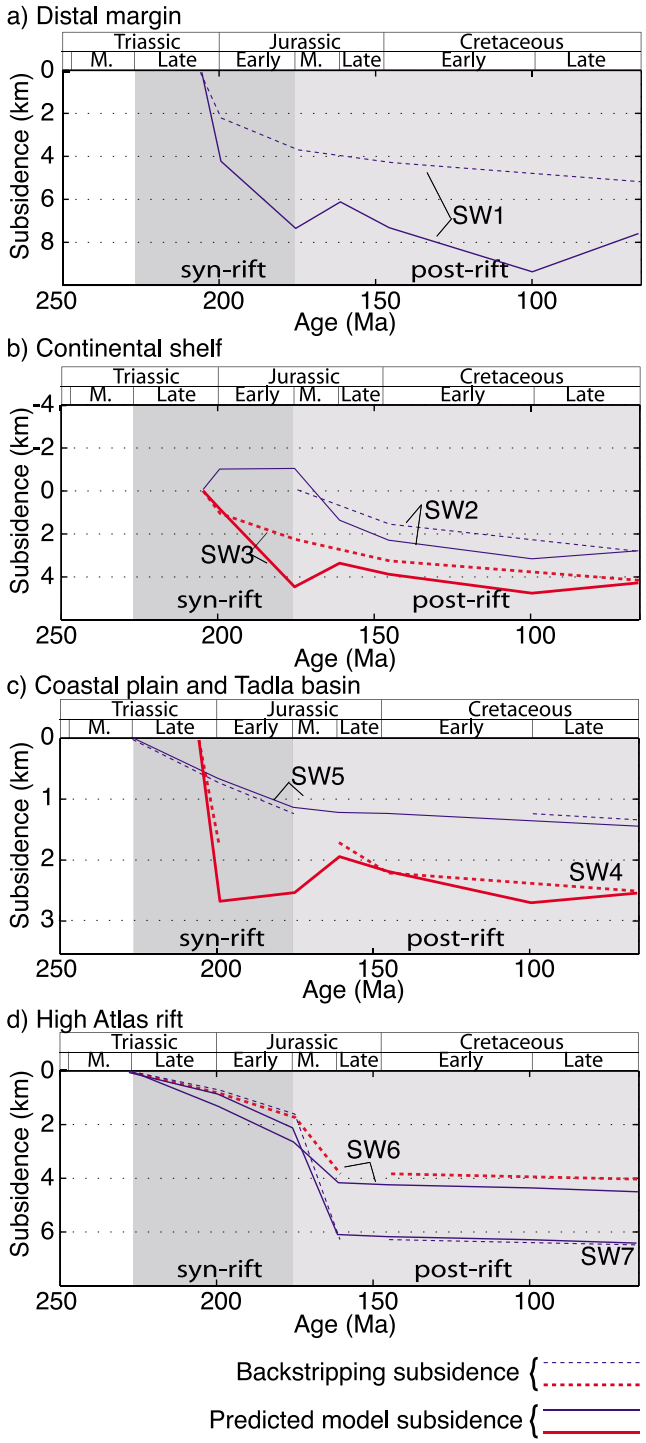

Figure 12. Subsidence curves extracted from the best fit model (solid lines) and comparison with backstripped subsidence curves (dashed lines).

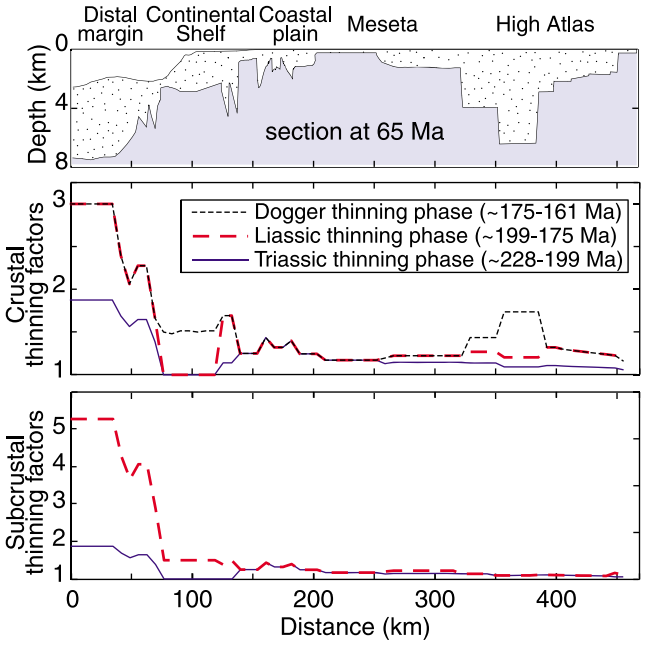

Figure 13. Crustal and subcrustal thinning factors for the 3 thinning phases adopted along the modeled transect: Triassic phase (228–199 Ma), Liassic phase (199–175 Ma) and Dogger phase (175–161 Ma). Partial thinning factors for each stage are determined by dividing the initial thickness (i.e., 33 km for the crust and 120 km for the lithosphere) by the thickness at the end of each phase.

significantly different from the observed one (Figure 14). More specifically, the model would predict strong Triassic and Liassic subsidence (up to 4 km and 6.4 km in the northern and central part of the Atlas, respectively) and an insignificant subsidence, almost zero, in the Dogger, which is in contradiction with the thick Dogger series observed in the Atlas.

[63] To explore the robustness of our assumption of a poly phase rift, we present two models with a single rifting episode with durations of 67 Myr (from 228 Ma to 161 Ma)

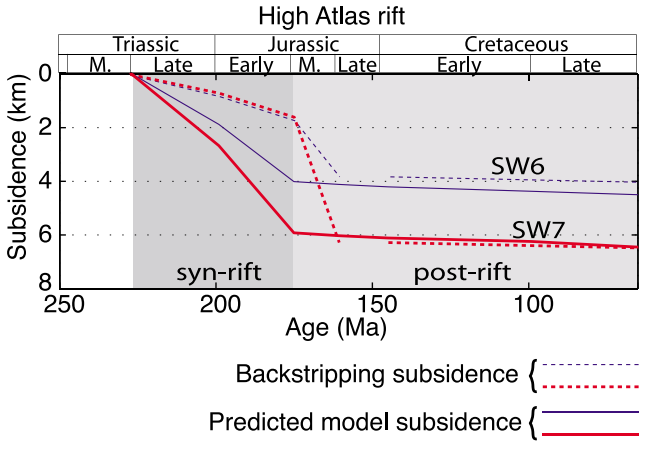

Figure 14. Predicted subsidence curves in the Atlas rift, for a model assuming two thinning phases, taking place in the Triassic and Lias, and comparison with the backstripped curves.

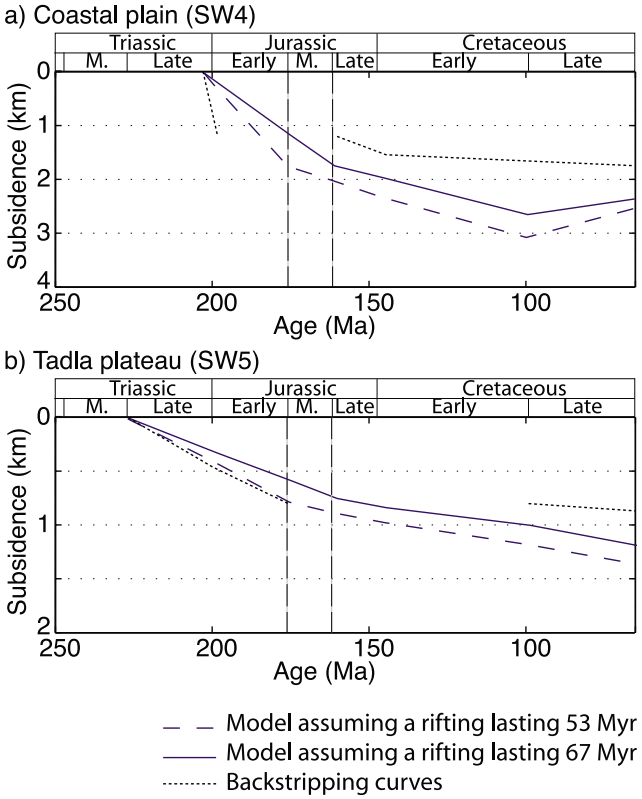

Figure 15. Predicted subsidence curves for models assuming one thinning phase (a) in the coastal plain (SW4) and (b) in Tadla plateau (SW5). Dashed lines mark subsidence curves inferred by backstripping and the solid lines indicate subsidence curve predicted by the model.

and 53 Myr (228 Ma to 175 Ma) and using the total thinning factors. Both models show a subsidence history significantly different than the observed one. The main differences are found in the coastal plain region and, less importantly, in the Tadla basin (Figure 15). In the coastal plain, the model predicts stronger-than observed downward movement from the Early Jurassic onwards. A too-strong subsidence is also predicted by the model in the Tadla basin. These findings provide a quantitative confirmation of the diachronous nature of continental rifting across NW Morocco.

5.4.2. Depth of Necking and Effective Elastic Thickness

[64] Changes in depth of necking have a profound influence on basement topography and, therefore, on basin architecture (Figure 16). A very shallow depth of 5 km produces topography much smoother than the observed one with too-shallow basins, as in the Atlas domain, and too-deep highs such as in the case of the Oualidia high. A deep necking depth of 30 km shows the opposite kind of deviations with too-deep basins, especially in the Atlas domain, and highs such as the Oualidia high and the Meseta which are predicted to be way above sea level.

[65] For necking depths similar to or lower than the best fit (15 km), changes in the isotherm describing the EET have limited impact on the basement topography (Figure 17a). Models with a larger depth of necking, in contrast, show more significant effects (Figure 17b). In this case, a relatively good fit can only be obtained with an EET defined by a cool isotherm (300°C), which corresponds to a low initial value of the effective elastic thickness (<27 km). The fit with observed basement architecture of the entire margin remains, however, poor.

5.4.3. Paleowater Depths in the Distal Margin

[66] Paleobathymetry is a very important parameter to model the subsidence of the deep part of the margin, where water depths as high as 5000 m are encountered. Paleowater depths are relevant only for the offshore part of the transect (i.e., the distal margin and the continental shelf), the other domains having remained at shallow water conditions during the evolution of the passive margin. All the models discussed before assume a linear increase of paleowater depths with time from 175 Ma (end of rifting) to the present-day, which would apply if the plate cooled and thickened indefinitely. To test a more realistic approach, we use a Sclater-type subsidence curve [*Sclater et al.*, 1980] for the oceanic crust to extrapolate paleowater depths in the distal margin (Figure 18). In this case, paleowater depths at 65 Ma would be of ~3800 m (against 2300 m using a linear evolution). The modeling results, using the same parameters as in the best fit model combined with Sclater-type

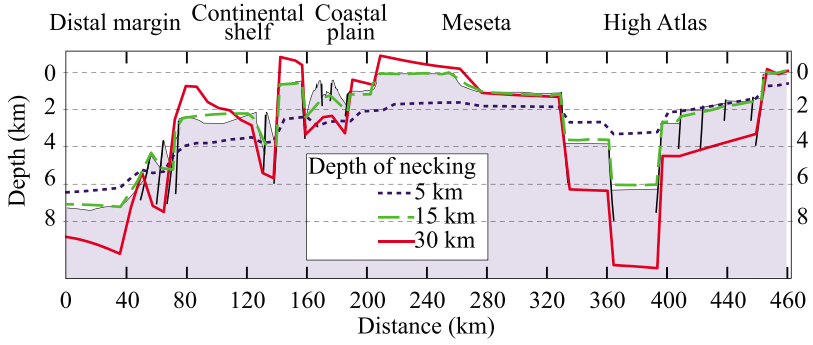

Figure 16. Reconstructed basement topography compared with predicted basement topography at the end of Cretaceous times, adopting necking depths of 5 km, 15 km (the best fit depth) and 30 km. The other parameters are the same as in the best fit model.

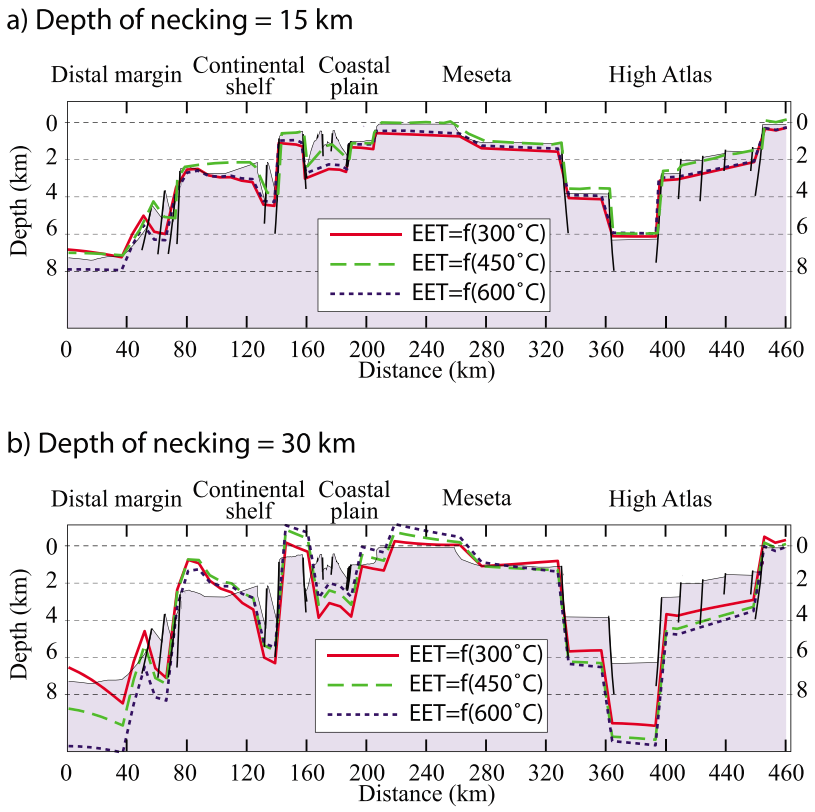

Figure 17. Predicted basement topography at the end of Cretaceous times for different isotherms describing the effective elastic thickness of the considered transect. (a) Adopted depth of necking is 15 km and (b) adopted depth of necking is 30 km. Other parameters are as for the best fit model.

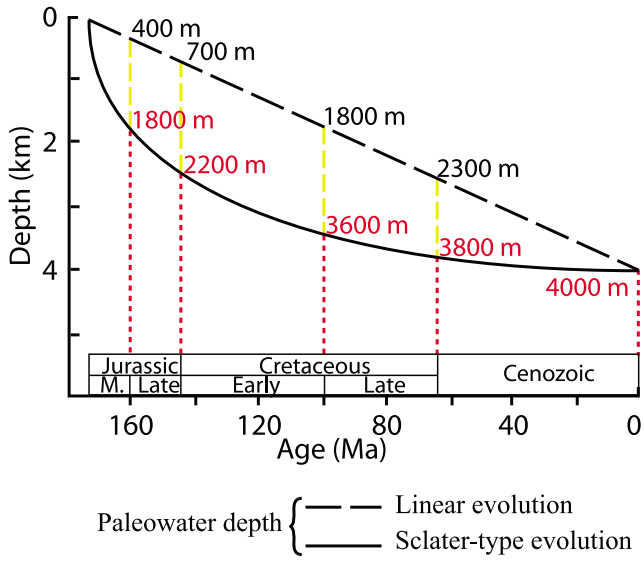

Figure 18. Paleowater depths evolution in the distal basin of the Doukkala-High Atlas margin. Dashed line represents a linear evolution with time and solid line shows a Sclater-type evolution (extrapolated from *Sclater et al.* [1980]).

paleowater depths, show that the basement topography at the end of the Cretaceous remains far above the expected depth (Figure 19). Indeed, the basement subsidence reaches only ~5 km in the distal margin, while it supposed to

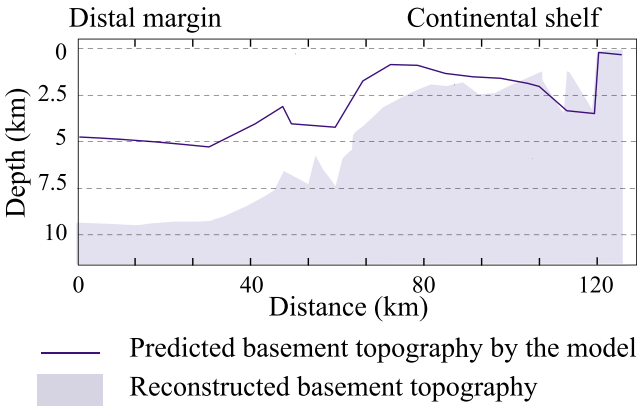

Figure 19. Predicted basement topography in the offshore margin for a configuration assuming the best fit model parameters combined with Sclater-type evolution paleowater depth.

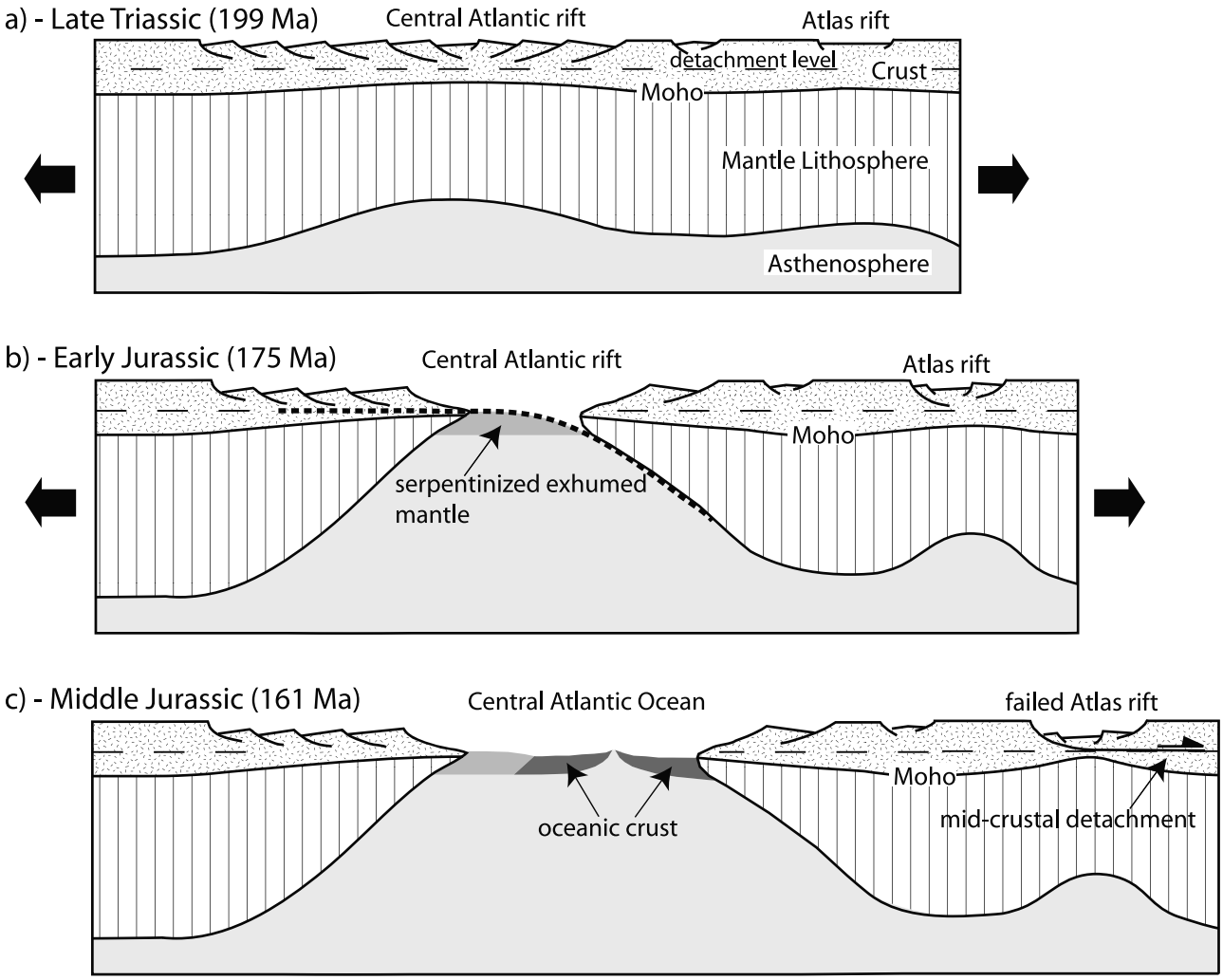

Figure 20. Conceptual rift model for the evolution of the Doukkala-High Atlas margin and conjugate eastern North American margin. (a) Initiation of distributed rifting along the transect. (b) Localization of rifting leading to mantle exhumation in the central part of the Atlantic rift (modified after *Maillard et al.* [2006]). (c) Ocean floor spreading in the Central Atlantic Ocean.

attain ~9 km to accommodate the 4 km-thick Mesozoic sediments.

6. Discussion

[67] Different geologic and kinematic scenarios of the rifted continental margin of NW Morocco have been tested in our models. The results provide an integrated analysis of the evolution of the entire margin, from the oceanic crust of the Central Atlantic to the High Atlas domain. The best fit model shows a good agreement between the large-scale (crustal and lithospheric) margin shape and stratigraphic architecture, and the constructed geologic section at 65 Ma. Our modeling work has a number of implications of importance for the evolution of the Moroccan margin in Mesozoic times.

6.1. Geometric Models of Rifting

[68] Our modeling results support the notion that rifting of the studied transect across the Moroccan passive margin occurred in three subsequent thinning phases: Late Triassic (228–199 Ma), Early Jurassic (199–175 Ma) and Middle Jurassic (175–161 Ma) (Figure 13), each phase being characterized by specific crustal and subcrustal thinning factors (Figure 13). Comparison between crustal and subcrustal thinning factors provides information on the geometry of rifting in the different phases addressing the question whether crustal thinning was accommodated in the same lithospheric column (pure shear geometry) or elsewhere (simple shear) [e.g., *Manspeizer*, 1988; *Bertrand*, 1991; *Favre and Stampfli*, 1992; *Laville et al.*, 1995; *Medina*, 1995].

[69] The first, Late Triassic, thinning stage (228–199 Ma) was characterized by comparable amounts of thinning in the crust and in the underlying subcrustal lithosphere (Figure 13) indicating pure shear geometry. This suggests efficient coupling between the crust and mantle lithosphere and the absence of significant rift-related thermal perturbations (Figure 20a). Thinning factors derived from the model in

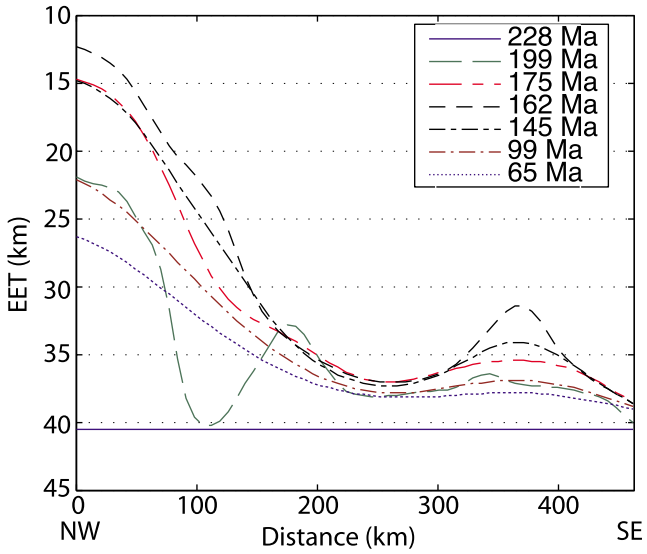

Figure 21. Evolution of the effective elastic thickness (EET) predicted by the best fit model for different ages.

this first stage are roughly comparable with those associated with fault-controlled extension. The overall Late Triassic setting is characterized by rifting taking place in several parts of the transect, namely the Atlantic margin and the Atlas system.

[70] Thinning during the Early Jurassic (i.e., second rift phase, 199–175 Ma) had also pure shear geometry with crustal and subcrustal thinning occurring in the same lithospheric column. In contrast with what deduced for the first stage, however, subcrustal thinning is significantly higher than the crustal one suggesting active rise of the asthenospehric mantle (Figure 20b).

[71] In the Middle Jurassic, i.e., third thinning phase (175–161 Ma), crustal thinning mostly affected the High Atlas rift and, less importantly, the continental shelf. Our best fit numerical model requires no coeval subcrustal thinning along the transect suggesting that crustal thinning was kinematically accommodated elsewhere. The results appear to support the idea that the late stages of rifting are accommodated by localized extension along a mid-crustal detachment in the Atlas domain [*Medina*, 1995; *Frizon de Lamotte et al.*, 2000; *Piqué et al.*, 2002] (Figure 20c). Obviously, the numerical model we use can only establish relations between subsidence and thinning without any consideration for other tectonic processes causing subsidence. Actually, the thinning needed to explain the observed subsidence is significantly larger than what can be associated with normal faulting (i.e., horizontal extension) known from the area. In a regional perspective, subsidence (thinning-related?) in the High Atlas was contemporaneous with thermal subsidence in the Atlantic margin.

6.2. Syn-Rift Strength of the Lithosphere

[72] Modeling results indicate that the lithosphere must have preserved some strength throughout rifting. According to our models, the Effective Elastic Thickness of the lithosphere is best described by the position of the 450°C isotherm. Figure 21 illustrates the vertical and lateral variations in the rigidity of the lithosphere along the margin through time. Predicted EET values are in the range of 40 km at the onset of rifting and reach 12 km in the distal margin by the end of rifting, indicating that the Moroccan lithosphere weakened but preserved some strength through rifting.

[73] The best fit model is obtained adopting a mid-crustal necking of the lithosphere (i.e., 15 km). The mechanical significance of the necking level has been interpreted in different ways [e.g., *Weissel and Karner*, 1989; *Kooi et al.*, 1992; *Van der Beek et al.*, 1994; *Spadini et al.*, 1995], considering the relationship between necking depths and detachment levels in the lithosphere and the presence or absence of strong layers in the pre-rift lithosphere. In the case of the Moroccan passive margin, no evidences of such a strong crustal layer is found in gravity [*Ayarza et al.*, 2005; *Zeyen et al.*, 2005; *Missenard et al.*, 2006] or seismic [*Contrucci et al.*, 2004] data. This level of necking might roughly correspond to the level of intracrustal detachment zones where the extensional listric faults sole out (Figure 22). A positive correlation between an increase in EET values and an increase in depth of necking is, thereby, observed by *Cloetingh et al.* [1995], indicating a link between these lithospheric strength indicators.

6.3. Anomalous Vertical Movements in the Central Part of the Doukkala-High Atlas Transect

[74] One of the most exciting discoveries made in the last few years on the geology of Morocco is the recognition that the Meseta block had not been stable and close to sea level during the Mesozoic as previously assumed but that it experienced Late Triassic to Early Jurassic subsidence followed by Middle Jurassic to Early Cretaceous exhumation [*Ghorbal et al.*, 2008; *Saddiqi et al.*, 2009]. In a tectonic perspective, these movements are peculiar as the Meseta block was bounded to the NW and SE by two basins (the Doukkala and Tadla basins) and had, therefore a horst position. Our modeling work documents the importance of flexurally driven vertical movements which could, therefore, take place in areas not directly affected by normal faulting. In locality SW4, for instance, the model predicts upward vertical movements during the Middle Jurassic (Figure 12c)

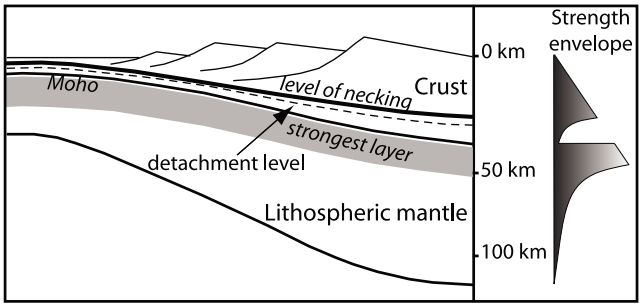

Figure 22. Interpretation of the mechanical significance of the level of necking (modified after *Van der Beek et al.* [1994]).

associated with the strong thinning in the coastal domains. Upward movement in the area of SW4 and to the E might have triggered erosion of the Meseta block and sustained consequent exhumation [e.g., *Burov and Cloetingh*, 1997]. Further field and modeling work is needed to test this hypothesis.

7. Conclusion

[75] The 450-km-long geological section we have constructed across the Central Atlantic continental margin of Morocco, the Meseta, the High Atlas Mountains and the adjacent part of the Anti-Atlas provides a quantitative description of the predominantly extensional structures which developed during and immediately following Central Atlantic rifting. The overall low amount of extension, ~20 km was accommodated by a number of extensional structures with lateral changes in onset and duration of tectonic activity.

[76] Numerical modeling results demonstrate that the observed stratigraphic record of the Doukkala-High Atlas transect can be reproduced assuming three continuous subsequent stages of lithospheric thinning, modulated by a depth-dependent effective elastic thickness defined by the 450°C isotherm and a level of necking which is 15 km deep. The lithosphere preserved a substantial strength during extension. The latter combined with the necking of the lithosphere largely explain the subsidence/uplift pattern observed in the different domains of the margin.

[77] Model results illustrate the diversity of lithosphere extension styles changing through time. Thereby, the pure shear prevailed in the 1st and 2nd phases, was followed by a localized simple shear in the 3rd phase.

[78] The kinematic-thermal model presented in this paper is able to reproduce most of the large-scale features of the investigated Doukkala-High Atlas margin. At the same time it provides the base for models which take into account the underlying physical processes of the rift phase and the rheological parameters of the thinned lithosphere.

[79] **Acknowledgments.** Our first acknowledgments go to the editor, the associate editor and the reviewers for constructive criticism that helped considerably to improve this article. We are grateful to M. El Moustaine and H. Jabour from ONHYM (Office National des Hydrocarbure et des Mines, Rabat/Morocco) who kindly provided us with the seismic data used in this work. We also acknowledge A. Kafif from the Moroccan Ministry of Energy and Mines for her help with the different geological maps of Morocco and Elishevah van Kooten for her support with the manuscript preparation.

References

Ait Brahim, L., et al. (2002), Paleostress evolution in the Moroccan African margin from Triassic to Present, *Tectonophysics*, *357*, 187–205, doi:10.1016/S0040-1951(02)00368-2.

Allen, P. A., and J. R. Allen (Eds.) (2005), *Basin Analysis: Principles and Applications*, 2nd ed., Blackwell Sci., Oxford, U. K.

Arboleya, M. L., A. Teixell, M. Charroud, and M. Julivert (2004), A structural transect through the High Atlas and Middle Atlas of Morocco, *J. Afr. Earth Sci.*, *39*, 319–327, doi:10.1016/j.jafrearsci.2004.07.036.

Ayarza, P., F. Alvarez-Lobato, A. Teixell, M. Arboleya, E. Tesón, M. Julivert, and M. Charroud (2005), Crustal structure under the central High Atlas Mountains (Morocco) from geological and gravity data, *Tectonophysics*, *400*, 67–84, doi:10.1016/j.tecto.2005.02.009.

Beauchamp, J. (1988), Triassic sedimentation and rifting in the High Atlas (Morocco), in *Triassic–Jurassic Rifting: Continental Breakup and the Origin of the Atlantic Ocean and Passive Margins, Dev. Geotecton. Ser.*, vol. 22, edited by W. Manspeizer, pp. 477–497, Elsevier, New York.

Beauchamp, W., R. Allmendinger, M. Barazangi, A. Demnati, M. El Alji, and M. Dahmani (1999), Inversion tectonics and the evolution of the High Atlas Mountains, Morocco, based on a geological-geophysical transect, *Tectonics*, *18*, 163–184, doi:10.1029/1998TC900015.

Benammi, M., E. A. Toto, and S. Chakiri (2001), Les chevauchements frontaux du haut atlas central marocain: Styles structuraux et taux de raccourcissement différentiel entre les versants nord et sud, *C. R. Acad. Sci.*, *333*, 241–247, doi:10.1016/S1251-8050(01)01628-7.

Bertotti, G., M. ter Voorde, S. Cloetingh, and V. Picotti (1997), Thermo-mechanical evolution of the South-Alpine rifted margin (North Italy): Constraints on the strength of passive continental margins, *Earth Planet. Sci. Lett.*, *146*, 181–193, doi:10.1016/S0012-821X(96)00214-2.

Bertrand, H. (1991), The Mesozoic tholeiitic province of Northwest Africa: A volcano-tectonic record of the early opening of the Central Atlantic, in *Magmatism in Extensional Structural Settings*, edited by B. A. Kampunza and R. T. Lubala, pp. 147–188, Springer, Berlin.

Bird, D. E., S. A. Hall, K. Burke, J. F. Casey, and D. S. Sawyer (2007), Early Central Atlantic Ocean seafloor spreading history, *Geosphere*, *3*, 282–298, doi:10.1130/GES00047.1.

Braun, J., and C. Beaumont (1987), Styles of continental rifting: Results from dynamic models of lithospheric extension, in *Sedimentary Basins and Basin-Forming Mechanisms*, vol. 36, edited by C. Beaumont and A. J. Tankard, pp. 241–258, Can. Soc. of Petrol. Geol, Calgary, Alberta, Canada.

Burov, E., and S. Cloetingh (1997), Erosion and rift dynamics: New thermomechanical aspects of post-rift evolution of extensional basins, *Earth Planet. Sci. Lett.*, *150*, 7–26, doi:10.1016/S0012-821X(97)00069-1.

Charrière, A. (1996), Contexte paléogéographique et paléotectonique de la formation des basins crétacés du Moyen-Atlas (Maroc) à la lumière des données stratiraphiques récentes, *Bull. Soc. Geol. Fr.*, *167*, 617–626.

Charrière, A., H. Haddouni, and P. O. Mojon (2005), Découverte de Jurassic supérieur et d'un niveau marin du Barrémien dans les "couches rouge" continentales du Haut Atlas central marocain: Implications paléogéographiques et structurales, *C. R. Palevol*, *4*, 385–394, doi:10.1016/j.crpv.2005.04.009.

Choubert, G., and A. Faure-Muret (1962), Evolution du domaine Atlasique Marocain depuis les temps paléozoïques, in *Livre à la Mémoire du Professeur Paul Fallot*, vol. 1, edited by D. Delga, pp. 447–527, Soc. Geol. Fr., Paris.

Cloetingh, S., J. D. van Wees, P. A. van der Beek, and G. Spadini (1995), Role of pre-rift rheology in kinematics of extentional basin formation: Constraints from thermomechanical models of Mediterranean and intracratonic basins, *Mar. Pet. Geol.*, *12*, 793–807, doi:10.1016/0264-8172(95)98848-Y.

Contrucci, I., F. Klingelhofer, J. Perrot, R. Bartolome, M. A. Gutcsher, M. Sahabi, J. Malod, and J. P. Rehault (2004), The crustal structure of the NW Moroccan continental margin from wide-angle and reflection seismic data, *Geophys. J. Int.*, *159*, 117–128, doi:10.1111/j.1365-246X.2004.02391.x.

Davison, I. (2005), Central Atlantic margin basins of North West Africa: Geology and hydrocarbon potential (Morocco to Guinea), *J. Afr. Earth Sci.*, *43*, 254–274, doi:10.1016/j.jafrearsci.2005.07.018.

Du Dresnay, R. (1987), Jurassic development of the region of the Atlas Mountains of Morocco: Chronology, sedimentation and structural significance, in *Geology and Culture of Morocco*, edited by C. D. Cornelius, M. Jarnaz, and E. P. Lehman, pp. 77–99, Earth Sci. Soc. Lybia, Tripoli.

Echarfaoui, H. (2003), Etude sismique du basin des Doukkala-Abda, Ph.D. thesis, Faculty of Sci., L'Univ. Ibn Tofail, Kenitra, Morocco.

El Arabi, E. H., J. B. Diez, J. Broutin, and R. Essamoud (2006), Première caractérisation palynologique du Trias moyen dans le Haut Atlas: Implications pour l'initiation du rifting téthysien au Maroc, *C. R. Geosci.*, *338*, 641–649, doi:10.1016/j.crte.2006.04.001.

El Harfi, A., J. Lang, J. Salomon, and E. Chellai (2001), Cenozoic sedimentary dynamics of the Ouarzazate foreland basin (Central High Atlas Mountains, Morocco), *Int. J. Earth Sci.*, *90*, 393–411, doi:10.1007/s005310000115.

El Harfi, A., M. Guiraud, and J. Lang (2006), Deep-rooted "thick skinned" model for the High Atlas Mountains (Morocco): Implications for the structural inheritance of the southern Tethys passive margin, *J. Struct. Geol.*, *28*, 1958–1976, doi:10.1016/j.jsg.2006.08.011.

Ellouz, N., M. Patriat, J.-M. Gaulier, R. Bouatmani, and S. Sabounji (2003), From rifting to Alpine inversion: Mesozoic and Cenozoic subsidence history of some Moroccan basins, *Sediment. Geol.*, *156*, 185–212, doi:10.1016/S0037-0738(02)00288-9.

Favre, P., and G. M. Stampfli (1992), From rifting to passive marging: The examples of the Red Sea, Central Atlantic and Alpine Tethys, *Tectonophysics*, *215*, 69–97, doi:10.1016/0040-1951(92)90075-H.

Frizon de Lamotte, D., J. Andrieux, and J. C. Guezou (1991), Cinématique des chevauchements Néogènes dans l'arc Bético-Rifain: Discussion sur les modèles géodynamiques, *Bull. Soc. Geol. Fr.*, *162*, 611–626.

Frizon de Lamotte, D., B. Saint Bèzard, R. Bracene, and E. Mercier (2000), The two main steps of the Atlas building and geodynamics of the western Med-

iterranean, *Tectonics*, *19*, 740–761, doi:10.1029/2000TC900003.

Frizon de Lamotte, D., et al. (2004), TRANSMED-Transect I: Betics, Alboran Sea, Rif, Moroccan Meseta, High Atlas, Jbel Saghro, Tindouf basin, in *The Transmed Atlas: The Mediterranean Region from Crust to Mantle*, edited by W. Cavazza et al., pp. 91–96, Springer, Berlin.

Frizon de Lamotte, D., M. Zizi, Y. Missenard, M. Hafid, M. El Azzouzi, R. C. Maury, A. Charriere, Z. Aki, M. Benammi, and A. Michard (2008), The Atlas system, in *Continental Evolution: The Geology of Morocco, Lect. Notes Earth Sci. Ser.*, vol. 116, edited by A. Michard, O. Saddiqi, and A. Chalouan, pp. 133–202, doi:10.1007/978-3-540-77076-3_4, Springer, Berlin.

Fullea, J., M. Fernandez, H. Zeyen, and J. Verges (2007), A rapid method to map the crustal and lithospheric thickness using elevation, geoid anomaly and thermal analysis: Application to the Gibraltar Arc System, Atlas Mountains and adjacent zones, *Tectonophysics*, *430*, 97–117, doi:10.1016/j.tecto.2006.11.003.

Ghorbal, B., G. Bertotti, J. Foeken, and P. Andriessen (2008), Unexpected Jurassic to Neogene vertical movements in 'stable' parts of NW Africa revealed by low temperature geochronology, *Terra Nova*, *20*, 355–363, doi:10.1111/j.1365-3121.2008.00828.x.

Giese, P., and V. Jacobshagen (1992), Inversion tectonics of intracontinental ranges: High and Middle Atlas, Morocco, *Geol. Rundsch.*, *81*, 249–259, doi:10.1007/BF01764553.

Gigout, M. (1965), Carte géologique de la Méséta entre Mechrâ Benâbbou et Safi (Abda, Doukkala et massif des Rhamna), *Notes Mem. Geol. Surv.*, *84*, scale 1:200,000, Geol. Serv. Morocco, Rabat, Morocco.

Hafid, M. (2000), Triassic-early Liassic extensional systems and their Tertiary inversion, Essaouira basin (Morocco), *Mar. Pet. Geol.*, *17*, 409–429, doi:10.1016/S0264-8172(98)00081-6.

Hafid, M. (2006), Styles structuraux du Haut Atlas de Cap Tafelney et de la partie sptentrionale du Haut Atlas Occidental: Tectonique salifère et relation entre l'Atlas et l'Atlantique, *Notes Mem. Geol. Surv. 465*, Geol. Serv. Morocco, Rabat, Morocco.

Hafid, M., M. Zizi, A. W. Bally, and A. Ait Salem (2006), Structural styles of the western onshore and offshore termination of the High Atlas, Morocco, *C. R. Geosci.*, *338*, 50–64, doi:10.1016/j.crte.2005.10.007.

Hafid, M., G. Tari, D. Bouhadioui, I. El Moussaid, H. Echarfaoui, A. Aït Salem, M. Nahim, and M. Dakki (2008), Atlantic basins, in *Continental Evolution: The Geology of Morocco, Lect. Notes Earth Sci. Ser.*, vol. 116, edited by A. Michard, O. Saddiqi, and A. Chalouan, pp. 303–329, doi:10.1007/978-3-540-77076-3_6, Springer, Berlin.

Hoepffner, C., A. Soulaimani, and A. Piqué (2005), The Moroccan Hercynides, *J. Afr. Earth Sci.*, *43*, 144–165, doi:10.1016/j.jafrearsci.2005.09.002.

Klitgord, K. D., and H. Schouten (1986), Plate kinematics of the Central Atlantic, in *The Western Atlantic Region*, vol. M, *The Geology of North America*, edited by P. R. Vogt and B. E. Tucholke, pp. 351–378, Geol. Soc. of Am., Boulder, Colo.

Kooi, H. (1991), Tectonic modeling of extentional basins: The role of lithospheric flexure, intraplate stress and relative sea-level change, Ph.D. thesis, VU Univ., Amsterdam.

Kooi, H., S. Cloetingh, and J. Burrus (1992), Lithospheric necking and regional isostasy at extensional basins; Subsidence and gravity modeling with an application to the Gulf of Lions margin (SE France), *J. Geophys. Res.*, *97*, 17,553–17,571, doi:10.1029/92JB01377.

Laville, E., and A. Piqué (1991), La distension crustale Atlantique et Atlasique au Maroc au début du Mésozoique: Le rejeu des structures hercyniennes, *Bull. Soc. Geol. Fr.*, *162*, 1161–1171.

Laville, E., and A. Piqué (1992), Jurassic penetrative deformation and Cenozoic uplift in the Central High Atlas (Morocco): A tectonic model, structural and orogenic inversions, *Geol. Rundsch.*, *81*, 157–170, doi:10.1007/BF01764546.

Laville, E., A. Charroud, B. Fedan, and A. Piqué (1995), Inversion négative et rifting Atlasique: L'exemple du bassin Triassique de Kerrouéne (Maroc), *Bull. Soc. Geol. Fr.*, *166*, 365–374.

Laville, E., A. Piqué, M. Amhar, and M. Charroud (2004), A restatement of the Mesoizoic Atlasic Rifting (Morocco), *J. Afr. Earth Sci.*, *38*, 145–153, doi:10.1016/j.jafrearsci.2003.12.003.

Le Roy, P. (1997), Les bassins ouest marocains: Leur formation et leur évolution dans le cadre de l'ouverture et du développement de l'Atlantique central (Marge Africaine), Ph.D. thesis, Univ. de Bretagne Occidentale, Brest, France.

Le Roy, P., and A. Piqué (2001), Triassic-Liaassic Western Moroccan synrift basins in relation to the Central Atlantic opening, *Mar. Geol.*, *172*, 359–381, doi:10.1016/S0025-3227(00)00130-4.

Maillard, A., J. Malod, E. Thiebot, F. Klingelhoefer, and J. P. Rehault (2006), Imaging a lithospheric detachment at the continent-ocean crustal transition off Morocco, *Earth Planet. Sci. Lett.*, *241*, 686–698, doi:10.1016/j.epsl.2005.11.013.

Manspeizer, W. (1988), A stratigraphic record from Morocco and North America of rifting, drifting and Tethyan transgressions of the central proto-Atlantic, *J. Earth Sci.*, *7*, 369–373, doi:10.1016/0899-5362(88)90081-4.

Medina, F. (1995), Syn- and postrift evolution of the El Jadida-Agadir basin (Morocco): Constraints for the rifting models of the Central Atlantic, *Can. J. Earth Sci.*, *32*, 1273–1291, doi:10.1139/e95-104.

Michard, A. (1976), Elément de Géologie Marocaine, *Notes Mem.Geol. Surv. 252*, Geol. Serv. Morocco, Rabat, Morocco.

Michard, A., D. Frizon de Lamotte, O. Saddiqi, and A. Chalouan (2008), An outline of the geology of Morocco, in *Continental Evolution: The Geology of Morocco*, *Lect. Notes Earth Sci. Ser.*, vol. 116, edited by A. Michard, O. Saddiqi, and A. Chalouan, pp. 1–31, doi:10.1007/978-3-540-77076-3_1, Springer, Berlin.

Missenard, Y., H. Zeyen, D. Frizon de Lamotte, P. Leturny, C. Petit, M. Sebrier, and O. Saddiqi (2006), Crustal versus asthenospheric origin of relief of the Atlas Mountains of Morocco, *J. Geophys. Res.*, *111*, B03401, doi:10.1029/2005JB003708.

Olsen, P. E. (1997), Stratigraphic record of the Early Mesozoic breackup of Pangea in the Laurasia-Gondwana rift system, *Annu. Rev. Earth Sci.*, *25*, 337–401, doi:10.1146/annurev.earth.25.1.337.

Péron-Pinvidic, G., and G. Manatschal (2009), The final rifting evolution at deep magma-poor passive margins from Iberia-Newfoundland: A new point of view, *Int. J. Earth Sci.*, *98*, 1581–1597, doi:10.1007/s00531-008-0337-9.

Piqué, A., D. Jeannette, and A. Michard (1980), The Western Meseta Shear Zone, a major permanent feature of the Hercynian belt in Morocco, *J. Struct. Geol.*, *2*, 55–61, doi:10.1016/0191-8141(80)90034-6.

Piqué, A., P. Tricart, R. Guiraud, E. Laville, S. Bouaziz, M. Amrhar, and R. Ait Ouali (2002), The Mesozoic-Cenozoic Atlas belt (North Africa): An overview, *Geodin. Acta*, *15*, 185–208, doi:10.1016/S0985-3111(02)01088-4.

Price, I. (1981), Provenance of the Jurassic-Cretaceous flysch, Deep Sea Drilling Project Sites 370 and 416, *Initial Rep. Deep Sea Drill. Proj.*, *50*, 751–757, doi:10.2973/dsdp.proc.50.139.1980.

Rimi, A. (1999), Mantle heat flow and geotherms for the main geologic domains in Morocco, *Int. J. Earth Sci.*, *88*, 458–466, doi:10.1007/s005310050278.

Ruellan, E. (1985), Géologie des marges continentales passives: Evolution de la marge Atlantique du Maroc (Mazagan); Etude par submersilble, Seabeam, et sismique reflexion, Ph.D. thesis, Univ. de Bretagne Occidentales, Brest, France.

Saddiqi, O., F.-Z. El Haimer, A. Michard, J. Barbarand, G. M. H. Ruiz, E. M. Mansour, P. Leturmy, and D. Frizon de Lamotte (2009), Apatite fission-track analyses on basement granites from south-western Meseta, Morocco: Paleogeographic implications and interpretation of AFT discrepancies, *Tectonophysics*, *475*, 29–37, doi:10.1016/j.tecto.2009.01.007.

Sahabi, M., A. Daniel, and J. L. Olivet (2004), Un nouveau point de départ pour l'histoire de l'Atlantique central, *C. R. Geosci.*, *336*, 1041–1052, doi:10.1016/j.crte.2004.03.017.

Schwarz, G., H. G. Mehl, F. Ramadi, and V. Rath (1992), Electrical resistivity structure of the eastern Moroccan Atlas System and its tectonic implications, *Geol. Rundsch.*, *81*, 221–235, doi:10.1007/BF01764551.

Sclater, J. G., C. Jaupart, and D. Galson (1980), The heat flow through oceanic and continental crust and the heat loss of the Earth, *Rev. Geophys.*, *18*, 269–311, doi:10.1029/RG018i001p00269.

Spadini, G., S. Cloetingh, and G. Bertotti (1995), Thermo-mechanical modeling of the Tyrrhenian Sea: Lithospheric necking and kinematics of rifting, *Tectonics*, *14*, 629–644, doi:10.1029/95TC00207.

Tadili, B., M. Ramadani, D. Ben Sari, K. Chapochnikov, and A. Bellot (1986), Structure de la croute dans le nord du Maroc, *Ann. Geophys.*, *4*, 99–104.

Tari, G., K. Marek, C. Miller, D. Valasek, and G. Walters (2007), Salt tectonics and play types, offshore Atlantic Morocco, paper presented at European Region Conference, Am. Assoc. of Pet. Geol., Athens, 18–21 Nov.

Teixell, A., M. L. Arboleya, M. Julivert, and M. Charroud (2003), Tectonic shortening and topography in the Central High Atlas (Morocco), *Tectonics*, *22*(5), 1051, doi:10.1029/2002TC001460.

Teixell, A., P. Ayarza, H. Zayen, M. Fernandez, and M. L. Arboleya (2005), Effects of mantle upwelling in a compressional setting: The Atlas Mountains of Morocco, *Terra Nova*, *17*, 456–461, doi:10.1111/j.1365-3121.2005.00633.x.

Van der Beek, P. A., S. Cloetingh, and P. A. M. Andriessen (1994), Mechanisms of extensional basin formation and vertical motions at rift flanks: Constraints from tectonic modeling and fission track thermochronology, *Earth Planet. Sci. Lett.*, *121*, 417–433, doi:10.1016/0012-821X(94)90081-7.

Van Houten, F. B. (1977), Triassic-Liassic deposits of Morocco and Eastern North America, *AAPG Bull.*, *61*, 79–99, doi:10.1306/C1EA3BFE-16C9-11D7-8645000102C1865D.

Van Wijk, J. W., and S. Cloetingh (2002), Basin migration caused by slow lithospheric extension, *Earth Planet. Sci. Lett.*, *198*, 275–288, doi:10.1016/S0012-821X(02)00560-5.

Verati, C., C. Rapaille, G. Feraud, A. Marzoli, H. Bertrand, and N. Youbi (2007), $^{40}Ar/^{39}Ar$ ages and duration of the Central Atlantic Magmatic Province volcanism in Morocco and Portugal and its relation to the Triassic–Jurassic boundary, *Palaeogeogr. Palaeoclimatol. Palaeoecol.*, *244*, 308–325, doi:10.1016/j.palaeo.2006.06.033.

Warme, J. (1988), Jurassic carbonate facies of the central and eastern High Atlas rift, Morocco, in *The Atlas System of Morocco*, edited by V. Jacobshagen, pp. 169–199, doi:10.1007/BFb0011593, Springer, Berlin.

Weissel, J. K., and G. D. Karner (1989), Flexural uplift of rift flanks due to mechanical unloading of the lithosphere during extension, *J. Geophys. Res.*, *94*, 13,919–13,950, doi:10.1029/JB094iB10p13919.

Wigger, P., G. Asch, P. Giese, W. D. Heinsohn, S. O. El Aalami, and F. Ramdani (1992), Crustal structure along a traverse across the Middle and High Atlas Mountains derived from seismic refraction studies, *Geol. Rundsch.*, *81*, 237–248, doi:10.1007/BF01764552.

Withjack, M. O., R. W. Schlische, and P. E. Olsen (1998), Diachronous rifting, drifting, and inversion on the passive margin of central eastern North America: An analog for other passive margins, *AAPG Bull.*, *82*, 817–835, doi:10.1306/1D9BC60B-172D-11D7-8645000102C1865D.

Withjack, M. O., R. W. Schlische, and P. E. Olsen (2010), Development of the passive margin of eastern North America: Mesozoic rifting, igneous activity, and breakup, in *Principles of Phanerozoic Regional Geology*, edited by D. G. Roberts and A. W. Bally, Elsevier, New York, in press.

Zeyen, H., P. Ayarza, M. Fernàndez, and A. Rimi (2005), Lithospheric structure under the western African-European plate boundary: A transect across the Atlas Mountains and the Gulf of Cadiz, *Tectonics*, *24*, TC2001, doi:10.1029/2004TC001639.

G. Bertotti and S. Cloetingh, Department of Tectonics and Structural Geology, VU University, De Boelelaan 1085, NL-1081 HV Amsterdam, Netherlands.

M. Gouiza, Netherlands Research Centre for Integrated Solid Earth Sciences, Department of Tectonics and Structural Geology, VU University, De Boelelaan 1085, NL-1081 HV Amsterdam, Netherlands. (mohammed.gouiza@falw.vu.nl)

M. Hafid, Département de Géologie, Faculté des Sciencces, L'Université Ibn Tofail, BP 133, 14000 Kenitra, Morocco.